European Journal of Medicinal Chemistry 128 (2017) 258–273

Contents lists available at ScienceDirect

European Journal of Medicinal Chemistry

journal homepage: http://www.elsevier.com/locate/ejmech

Research paper

Tetrazolylmethyl quinolines: Design, docking studies, synthesis, anticancer and antifungal analyses

Saba Kauser J. Shaikh [a], Ravindra R. Kamble [a, *], Shilpa M. Somagond [a], H.C. Devarajegowda [b], Sheshagiri R. Dixit [c], Shrinivas D. Joshi [c]

[a] Department of Chemistry, Karnatak University Dharwad, Pavate Nagar, Dharwad, 580 003, Karnataka, India
[b] Department of Physics, Yuvaraja's College, University of Mysore, Mysore, 570 005, Karnataka, India
[c] Novel Drug Design and Discovery Laboratory, Department of Pharmaceutical Chemistry, S.E.T.'s College of Pharmacy, Sangolli Rayanna Nagar, Dharwad, 580 002, Karnataka, India

ARTICLE INFO

Article history:
Received 28 October 2016
Received in revised form
25 January 2017
Accepted 28 January 2017
Available online 1 February 2017

Keywords:
Quinoline
Tetrazole
Regioisomer
Molecular docking
DNA
N-Myristoyl transferase
Dihydrofolate reductase
Anticancer activity
Antifungal screening

ABSTRACT

A new series of 2,5 and 1,5-regioisomers of the tetrazolyl group *viz*., 3-[(5-benzyl/benzylthio-2*H*-tetrazol-2-yl) methyl]-2-chloro-6-substituted quinoline **6h-q** and 3-[(5-benzyl/benzylthio-1*H*-tetrazol-1-yl) methyl]-2-chloro-6-substituted quinolines **7h-q** were synthesized. Docking studies of all these compounds with DNA as target using PDB: 1AU5 and 453D revealed that the compounds **6h** and **6i** act as covalent cross linker on the DNA helix of the former and intercalate the latter both with higher C score values. Another set of docking studies in the active pocket of dihydrofolate reductase and *N*-myristoyl transferase as targets to assess antifungal activity revealed that compounds **6k**, **6l**, **6p** and **7q** (with *bromo* and *fluro* substituents) showcases different binding modes and hydrogen bonding. Further, the compounds were screened for anticancer activity (primary cytotoxicity) against NCI-60 Human tumor cell line at a single high dose (10^{-5} M) concentration assay. Among the tested compounds, **6h** has shown 99.28% of GI against Melanoma **(SK-MEL-5)** and compound **6i** has shown 97.56% of GI against Breast Cancer **(T-47D)**. Further, *in vitro* antifungal assay against *A. fumigatus* and *C. albicans* for these compounds **6h-q** and **7h-q** revealed potential to moderate activities as compared to the standard.

1. Introduction

Cancer is one of the second leading causes of mortality, which is a great concern of the current century to the mankind. Moreover, all the countries across the globe are being increasingly affected with this disease. As the populations live longer, the negative lifestyle and the food habits also increase the cancer risk, which conveys that cancer can also be termed as lifestyle disease. As per the world cancer report released by WHO in the forthcoming years the mortality rates due to cancer will increase twice its current percentage [1,2]. Therefore, discovery and development of newer anticancer agents have become the need and the key focus of many researchers and pharmaceutical companies. Although earlier reported chemotherapeutic drugs efficiently kill cancer cells, but many times this concludes to develop multi-drug resistance [3]. Prevalence of fungal infections is increasing over the past few years by an increase in cases which are susceptible to such pathogenic infections. These include patients undergoing chemotherapy for cancer, malignancies, AIDS or immunosuppressed by afflictions, with high risk of getting fungal infections [4]. However, like bacterial infections, some fungi no longer respond to the antifungal medications which were designed to cure them and most of the marketed antifungal agents have several drawbacks with respect to the potency and spectrum of activity. These factors motivate the researchers to design and develop novel targets with effective mode of mechanism, more bioactivity and least side effects [5].

Quinoline and its derivatives are considered to be versatile synthetic modules since they have shown modes of action in the inhibition of tyrosine kinases; proteasome, tubulin polymerization and DNA repair [6]. Quinoline nucleus also occurs in several natural compounds and it is one of the pharmacologically active substances displaying a wide range spectrum of biological activity. The scaffold can also be found in many classes of biologically active compounds such as antibacterials, antiprotozoic drugs [7–10], anti-tubercular

* Corresponding author.
E-mail address: kamchem9@gmail.com (R.R. Kamble).

http://dx.doi.org/10.1016/j.ejmech.2017.01.043
0223-5234/

agents [11–14], antiprion [15] and anticancer agents [16–23]. Some quinoline analogues also showed antifilarial and HIV integrase inhibitory activities [24,25] which make it to be a valuable scaffold for many biologically active compounds and several marketed drugs [26]. Tetrazole, a five membered heterocycle is considered as a bioisostere of carboxylic group and is a pharmacophore possessing wide range of biological activities. Several substituted tetrazoles have been shown to possess anticonvulsant [27], antibacterial [28,29], anti-inflammatory [30,31], antinociceptive [32,33], anticancer [34,35], cyclo-oxygenase inhibition [36] and hypoglycemic activities [37]. It has also been reported that the lipophilic nature of tetrazole moiety in a drug improves its oral bioavailability and cell penetration [38]. One of the marketed analgesic compound, Alfentanil **i** contains a tetrazolone moiety and on the other hand TAK-456 **ii** with tetrazole ring has a broad-spectrum antifungal activity [39] Fig. 1a.

Docking is a method which predicts the orientation of one macromolecule of protein to the ligand when bound to each other, thus forming a stable complex at the atomic level [40]. Actually, drug discovery program is oriented towards the search for lead structures and thus virtual screening/molecular docking program constitute a great tool to find hit which further undergoes limited optimization to identify promising lead molecule. In the present paper, we have carried out docking of the compounds **6h-q** and **7h-q** into the base pairs of DNA and active sites of *N*-myristoyl transferase (NMT) and dihydrofolate reductase (DHFR). This is because DNA being specifically taken as a molecular target for many of the clinically available drugs which is trending in cancer therapeutics and is a non-specific target of cytotoxic agents. It was noticed that smaller drug molecules which contain planar polyaromatic systems bind to double stranded DNA and exhibit more than one binding mode *ie.*, the intercalation and covalent binding. It has been oriental as a target for many antitumor as well as antibiotic drugs and hence further interaction of drug and DNA is important to study the rational designing of selective targets in pharmacology [41,42]. NMT is a cytosolic monomeric enzyme that catalyzes the transfer of

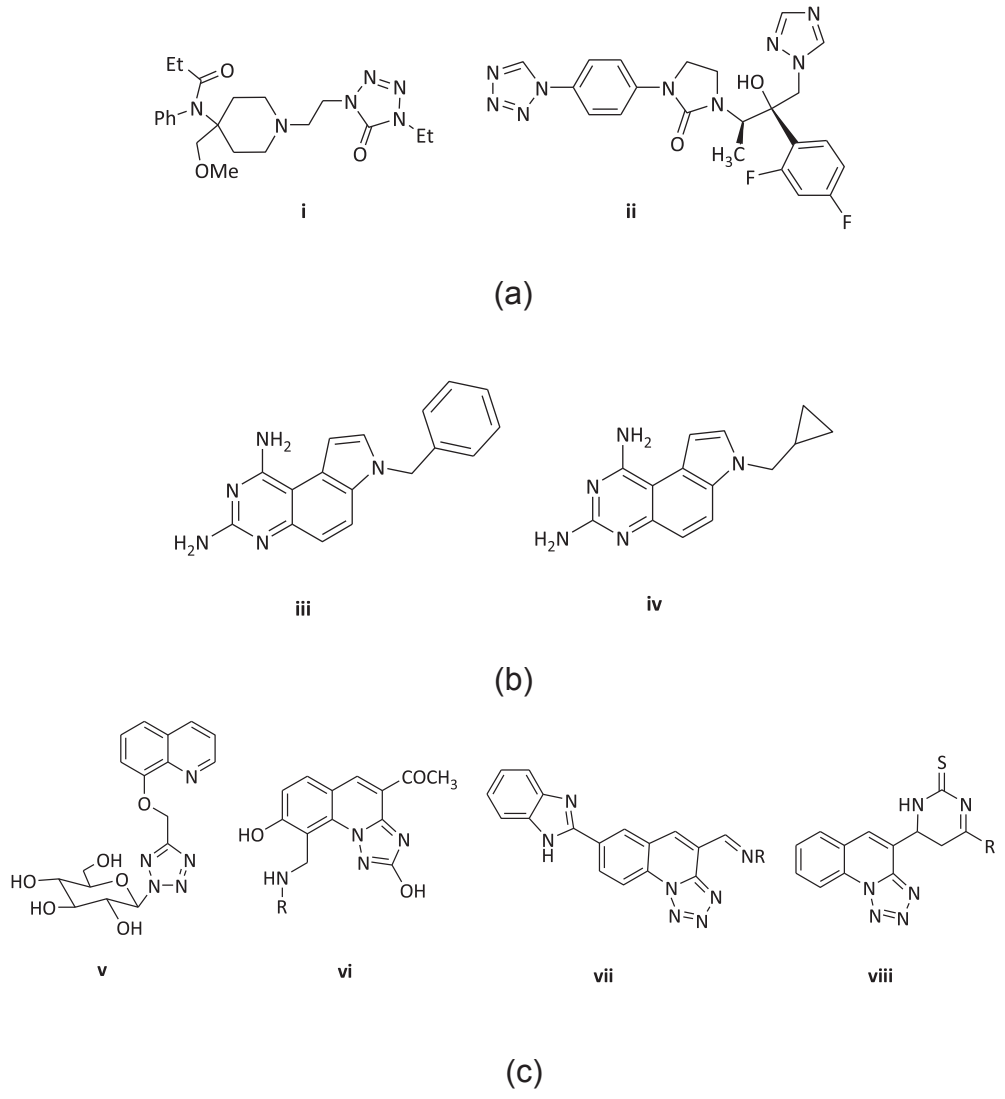

Fig. 1. (a) Marketed drugs containing tetrazole moiety. (b) *C. albicans* inhibiting Quinazolines. (c) Anticancer and antifungal azole quinolines.

the myristoyl group from myristoyl-CoA to the N-terminal glycine of a number of eukaryotic cellular and viral proteins [43,44]. Although *A. fumigatus* possess an active NMT enzyme, genetic studies have shown that NMT gene is essential for the growth and viability of important pathogenic fungi including *C. albicans* [45]. Hence, NMT is an important and promising target enzyme in the design and development of novel antifungal agents. By earlier reports, NMT has also been known to be a promising target of anticancer agents and also a large number of potent NMT inhibitors showing antifungal, antiparasitic activities have been reported [46].

DHFR catalyzes the reduction of dihydrofolic acid to tetrahydrofolic acid *viz*., involved in the biosynthesis of DNA. Therefore, inhibition of DHFR causes the cessation of DNA synthesis which ultimately leads to cell death. This enzyme is target of intervention for a number of well-known drugs *viz*., the antibacterial agent Trimethoprim and the anticancer agent Methotrexate [47]. Interestingly, DHFR inhibitors have also shown *in vitro* antifungal activity. For example, pyrrolo-2,4-diaminoquinazolines **iii** and **iv** have shown potent activity against *C. albicans* Fig. 1b [48,49].

Thus, the fusion of quinoline to the tetrazole ring is speculated to increase the biological activity. This prompted us to design and construct a system containing tetrazole ring with the quinoline matrix to serve as a new scaffold for the synthesis of anticancer agents **v-vi** [50,51] and antifungals **vii-viii** represented in Fig. 1c [52,53].

The designed compounds consist of a quinoline nucleus which serves as pharmacophore and the non-heterocyclic part *viz*., phenyl group separated by a tetrazole bridge represents the linker as shown in Fig. 2. Due to the planarity, there is more hydrogen bond environment with tetrazolates as indicated by computational data [54]. The *pKa* value of tetrazole is more than carboxylic surrogates which makes it a lipophilic part for oral bioavailability and improved duration of action. Substituents at the 6th position on the core moiety *i.e*., quinoline rationally increases the activity of the scaffold as a whole [55]. All these observations lead us to design the molecules as shown in Fig. 2.

These observations have also been substantiated by molecular docking with DNA and into the active sites of NMT (*A. fumigatus*) and DHFR (*C. albicans*) as targets. The docking studies have been further corroborated by *in vitro* analyses.

2. Results and discussion

2.1. Pharmacology

2.1.1. DNA docking simulation

Docking studies were carried out on Surflex-Dock program which is a surface-based molecular similarity wherein ligands were docked into the protein to optimize the value of the scoring function. Since DNA is the target for many of the drugs used in cancer therapeutics, the study was performed on both PDB 1AU5 and PDB 453D to support the interaction and preferred binding mode of compounds **6h-q** and **7h-q** with DNA. The protein crystal structures were obtained from the PDB (www.rcsb.org/pdb).

The docking study on PDB 1AU5 revealed that compounds **6h** and **6i** act as covalent cross linkers, as they showed covalent cross-linking mode of binding with the base pairs of DNA helix structure PDB 1AU5. As depicted in Fig. 3**(a)**, compound **6h** showed covalent cross-linkage mode of binding with the base pair of DNA helix, while the nitrogen of tetrazole ring forms a weak hydrogen bond with hydrogen of DC12 base pair. Also in Fig. 3 **(b)**, the compound **6i** showed the same mode of binding as that of compound **6h**, makes four hydrogen bonding interaction. Two nitrogen of tetrazole ring makes three hydrogen bonds, one with DA11 base pair, two with DC 12 base pairs and another one is from the oxygen atom of the methoxy group at 6th position of the quinoline ring with hydrogen of DA14 base pair. On the other hand, the docking study on PDB 453D revealed that compounds **6h** and **6i** act as intercalator (See Fig. 4).

As depicted in Fig. 5 **(a)** and **(b)**, they may undergo threading or classical intercalation. This observation also substantiated the *in vitro* anticancer screening wherein, these two compounds exhibited potent activity. The predicted binding energies of all the compounds on PDB 1AU5 are listed in Table 1 which shows that the compound **6h** and **6i** exhibits the highest C-score values of 4.19 and 3.94 which is in agreement with our observed *in vitro* results. The binding energies of titled compounds on PDB 453D are provided (Table No. S19, Supplementary Information) (see Fig. 6).

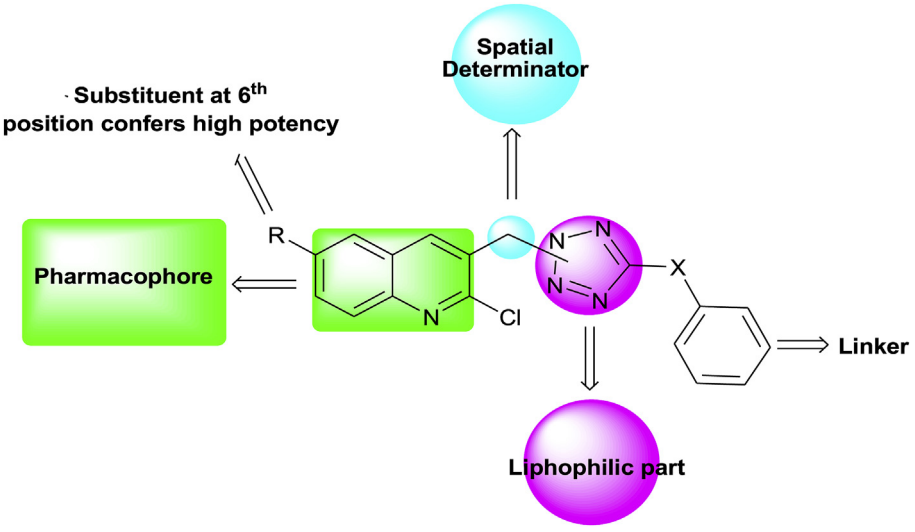

Fig. 2. SAR based design of title compounds.

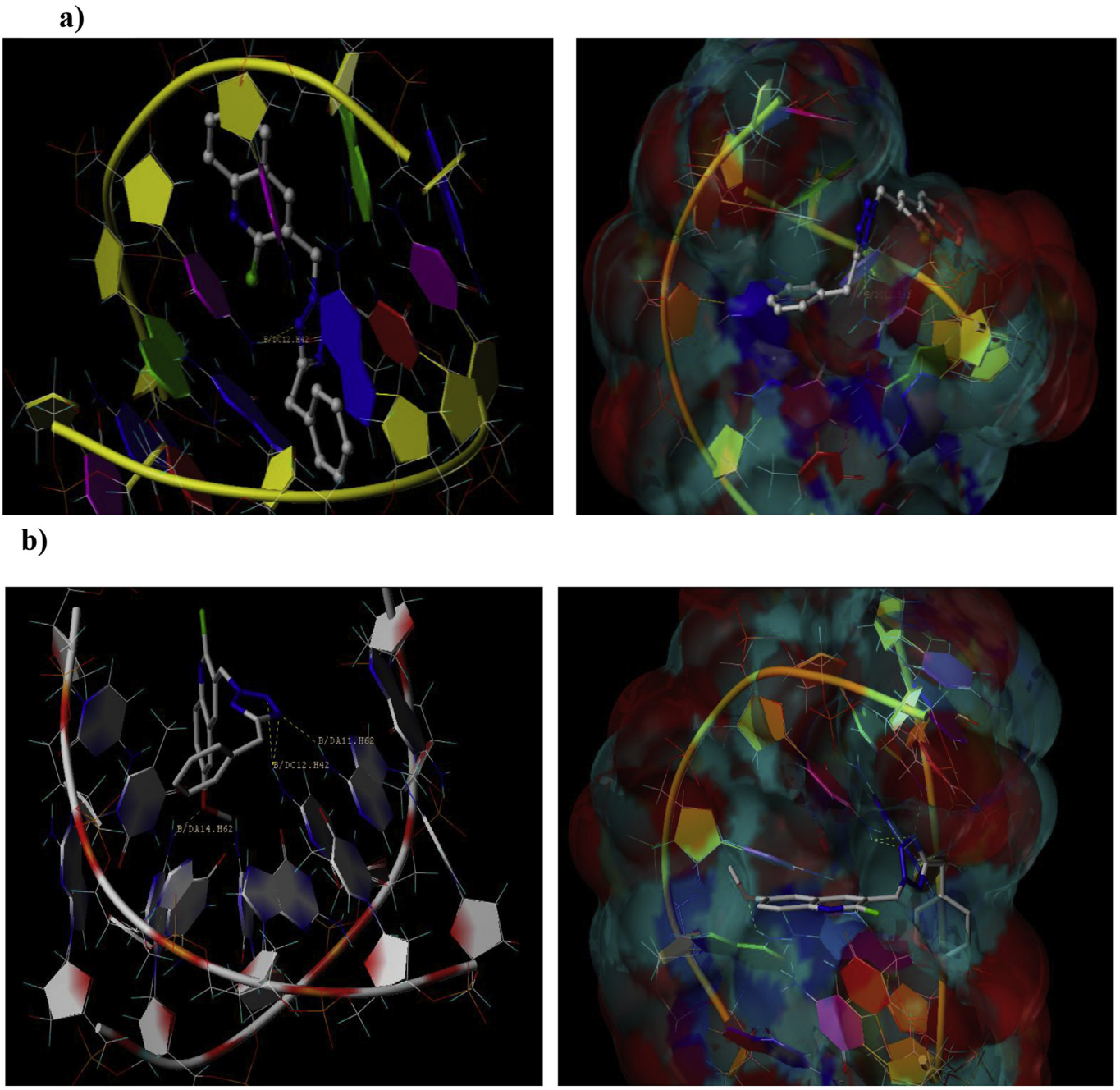

Fig. 3. **(a)** 3D binding model of compound **6h** docked into the active pocket of PDB: 1AU5, **(b)** 3D binding model of compound **6i** docked into the active pocket of PDB: 1AU5.

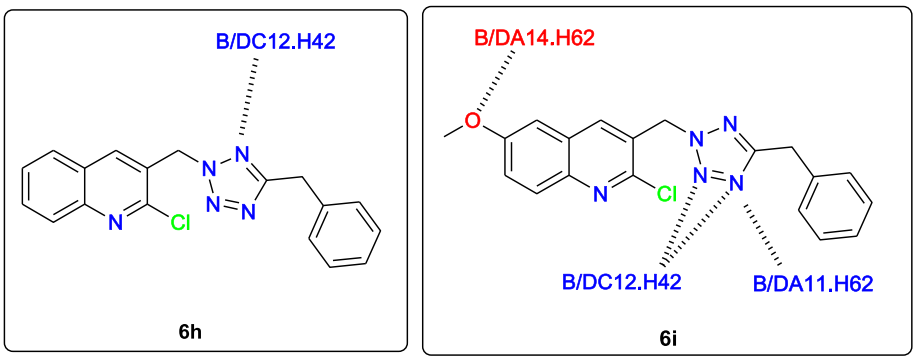

Fig. 4. Binding interactions of **6h** and **6i** at the active site of PDB 1AU5.

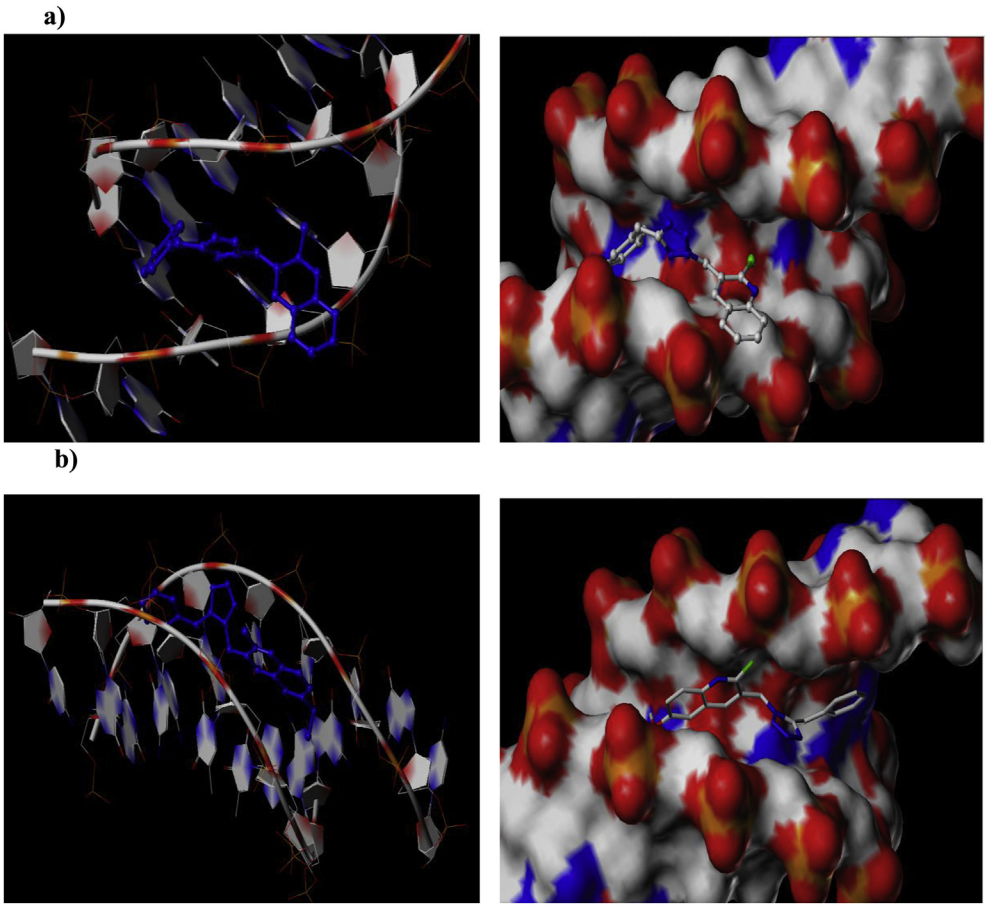

Fig. 5. **(a)** Interaction of compound **6h** at the binding site of PDB 453D, **(b)** Interaction of compound **6i** at the binding site of PDB 453D.

2.1.2. Molecular docking studies against NMT and DHFR

The orientation of inhibitor bound in the active sites of both NMT and DHFR as templates to study antifungal activity against *A. fumigatus* and *C. albicans* respectively was ascertained by docking study. The protein crystal structure file (PDB ID: 4CAW; B-Chain and 1AI9) was taken from PDB (www.rcsb.org/pdb). The molecular docking studies suggested that all the tested compounds show different binding modes with the active site of one or more amino acids through hydrogen bonding in the active pocket of the enzyme. The study revealed that the compounds **6k**, **6l**, **6p** and **7q** show exceptional interaction against NMT and DHFR. As shown in Fig. 7 **(a)**, compound **6k** formed four hydrogen bonds and its C score and Crash score are 7.14 and −1.58 kcal/mol and is considered to be a good inhibitor of DHFR (PDB: 1AI9). The nitrogen atom at 5th position of the tetrazole ring in compound **6k** makes one hydrogen bonding interaction with amino acid residue ILE96 (N———H.ILE96; 2.43 Å) and remaining three interactions came from the nitrogen atom present at 2nd position of tetrazole ring which make two hydrogen bonding interactions with hydrogen of ARG79 (N—H.ARG79; 2.14 Å and 2.33 Å) and lastly nitrogen atom of quinoline ring makes hydrogen bonding interaction with ARG79 (N—H.ARG79; 2.07 Å).

As the depicted in Fig. 7 **(b)**, compound **7q** revealed one hydrogen bond and its C score and Crash score are 5.76 and −1.31 kcal/mol and is considered to be a good inhibitor of NMT (PDB ID: 4CAW) to exhibit the activity against *A. fumigatus*. A nitrogen atom of quinoline ring makes hydrogen bonding interaction with SER378 (N——H.SER378; 2.11 Å). The C-score (Consensus score) indicated the summary of all the forces interacted between the ligands and enzyme. Crash score revealed that probable penetration into the binding site was in favor of ligands under study. Charge and van der Waals interactions between the protein and the ligand suggested that compounds **6k**, **6l**, **6p** and **7q** are versatile compared to other ligands. Scoring of compounds with respect to the reward for hydrogen bonding, lipophilic contact, and rotational entropy, along with, intercept terms revealed that compounds **6k**, **6l**, **6p** and **7q** showed increased interactions with the protein than other compounds. The binding energies of titled compounds on enzyme DHFR (Table No. S20, Supplementary Information) and NMT (Table No. S21, Supplementary Information) are provided.

2.2. Chemistry

Benzyl/Benzylthio tetrazole **2a-b** was prepared as per Scheme 1. 2-Chloro-6-substituted-quinoline-3-carbaldehyde **3c-g** was prepared by *Vilsmeier-Haack* reaction which further was reduced using $NaBH_4$ to the corresponding alcohol **4c-g**. This later gave 3-(bromomethyl)-2-chloro-6-substituted quinoline **5c-g** when treated with phosphorous tribromide in DCM. *N*-Alkylation of 5-substituted tetrazole **2a-b** with 3-(bromomethyl)-2-chloro-6-substituted quinoline **5c-g** in presence of anhydrous potassium carbonate led to the formation of regioisomers 3-[(5-benzyl/benzylthio-2*H*-tetrazol-2-yl) methyl]-2-chloro-6-substituted quinoline **6h-q** and 3-[(5-benzyl/benzylthio-1*H*-tetrazol-1-yl) methyl]-2-chloro-6-substituted quinoline **7h-q** in almost 1:1 ratio at room temperature at 76–92% yields Scheme 2. Also, literature reports revealed that, 5-substituted tetrazole forms 1*H* and 2*H*-tautomers Fig. 8.

Table 1
Surflex docking scores (kcal/mol) of the titled compounds **6h-q** and **7h-q** on PDB 1AU5.

Compound	C Score[a]	Crash Score[b]	Polar Score[c]	D Score[d]	PMF Score[e]	G Score[f]	Chem Score[g]
6h*	4.19	−1.01	2.07	−133.78	−83.57	−172.04	−18.18
6i*	3.94	−0.99	0.87	−135.80	−77.78	−192.66	−15.80
6j	3.56	−0.52	1.10	−115.40	−69.77	−146.53	−11.38
6k	3.30	−0.73	1.31	−125.46	−41.12	−153.76	−12.53
6l	3.88	−0.86	2.12	−127.79	−85.31	−149.54	−17.50
6m	2.61	−0.75	0.21	−121.94	−68.45	−160.62	−10.85
6n	3.23	−0.70	0.80	−137.84	−86.13	−164.12	−14.94
6o	3.65	−0.82	0.10	−131.18	−44.86	−161.71	−12.23
6p	2.95	−0.75	0.01	−121.94	−68.45	−160.62	−10.85
6q	3.10	−0.89	0.71	−134.95	−98.31	−172.21	−12.43
7h	3.84	−0.59	0.20	−122.35	−69.11	−168.63	−11.83
7i	2.92	−0.49	2.17	−123.67	−82.88	−149.67	−17.66
7j	2.81	−0.76	0.82	−123.87	−70.37	−158.72	−10.93
7k	2.79	−0.80	1.00	−132.95	−64.77	−178.45	−12.24
7l	2.48	−0.53	0.81	−107.17	−65.85	−131.46	−11.92
7m	2.24	−0.61	0.43	−134.04	−67.68	−172.32	−11.01
7n	2.97	−0.78	0.34	−123.24	−55.74	−152.43	−12.50
7o	2.84	−0.37	0.62	−137.59	−51.74	−171.33	−13.66
7p	3.24	−0.52	0.01	−129.99	−58.74	−147.65	−13.88
7q	3.70	−0.62	0.04	−120.59	−65.59	−157.49	−10.93

*Asterisk indicates the compound with highest C Score.
[a] C-Score (Consensus Score) integrates a number of popular scoring functions for ranking the affinity of ligands bound to the active site of a receptor and reports the output of total score.
[b] Crash-score revealed the inappropriate penetration into the binding site. Crash scores close to 0 are favorable. Negative numbers indicate penetration.
[c] Polar is indicating the contribution of the polar interactions to the total score. The polar score may be useful for excluding docking results that make no hydrogen bonds.
[d] D-score for charge and van der Waals interactions between the protein and the ligand.
[e] PMF-score indicating the Helmholtz free energies of interactions for protein-ligand atom pairs (Potential of Mean Force, PMF).
[f] G-score showing hydrogen bonding, complex (ligand-protein), and internal (ligand-ligand) energies.
[g] Chem-score points for H-bonding, lipophilic contact, and rotational entropy, along with an intercept term.

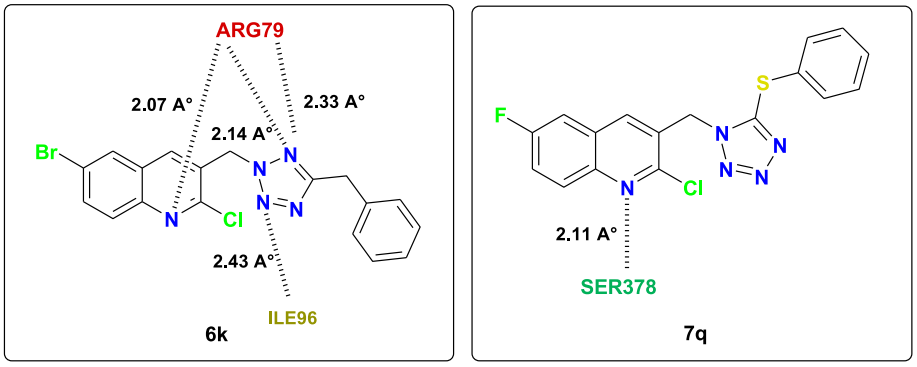

Fig. 6. Binding interactions of **6k** into the active site of the enzyme DHFR and **7q** into the active site enzyme NMT.

In order to obtain only one isomer *i.e.*, 2,5-isomer **6h-q** we attempted *Buchwald-Hartwig* coupling reaction [56]. For this, precursor **8a-b** was prepared by [3 + 2] cycloaddition of nitriles with tributyltin azide. The azide was generated *in situ* from tributyltin chloride and sodium azide, and the palladium-based coupling of **8a-b** was attempted with 3-(bromomethyl)-2-chloro-6-substituted quinoline **5c-g** as a substrate in presence of base (anhydrous K_2CO_3) in dry THF under N_2 atmosphere for 24 h Scheme 3. However, on monitoring the reaction we found, instead of formation of compound **6h-q** as the sole product, there was formation of both the regioisomers. This was because base such as potassium carbonate removed the acidic proton of tetrazole and formed anion as shown in Scheme 4. This led to the formation of both the isomers due to failure in the completion of coupling cycle. This in turn resulted in failure of *regioselectivity* during the reaction process.

The regioisomers **6h-q** and **7h-q** were analyzed by LC-MS which indicates that the two isomers are in almost equal proportions. Later, the regioisomers were eluted in the ratio 1:1. The structures of these compounds were confirmed by ^1H, ^{13}C NMR, mass spectra, X-ray crystallography and elemental analyses. A medium intense band appeared in all the compounds around 1589-1625 cm^{-1} correspond to the C=N stretching. In case of ^1H NMR, the C_4-H of the quinoline ring appeared as a singlet around 8.08–8.59 ppm. In case of 2,5-regioisomer, the N-CH_2 protons flanked between quinoline and tetrazolyl ring resonate as a singlet around 6.15–6.10 ppm. Similarly, in case of 1,5-regioisomer these N-CH_2 protons resonate at 5.76–6.11 ppm. The C-CH_2-C protons resonate as a singlet at 4.08–4.36 ppm in case of 2,5-regioiosmer and at 4.19–4.55 ppm for 1,5-regioisomer. The signals appeared around 7.03–7.48 ppm was attributed to the aromatic protons in all the compounds. In case of ^{13}C NMR spectral analyses, the C_5 carbon of tetrazolyl ring resonated around 165-154 ppm and the other magnetically non equivalent carbon atoms appeared as signals at their respective chemical shift values. The mass spectral analyses of all the title compounds have shown the molecular ion peak corresponding to their molecular mass.

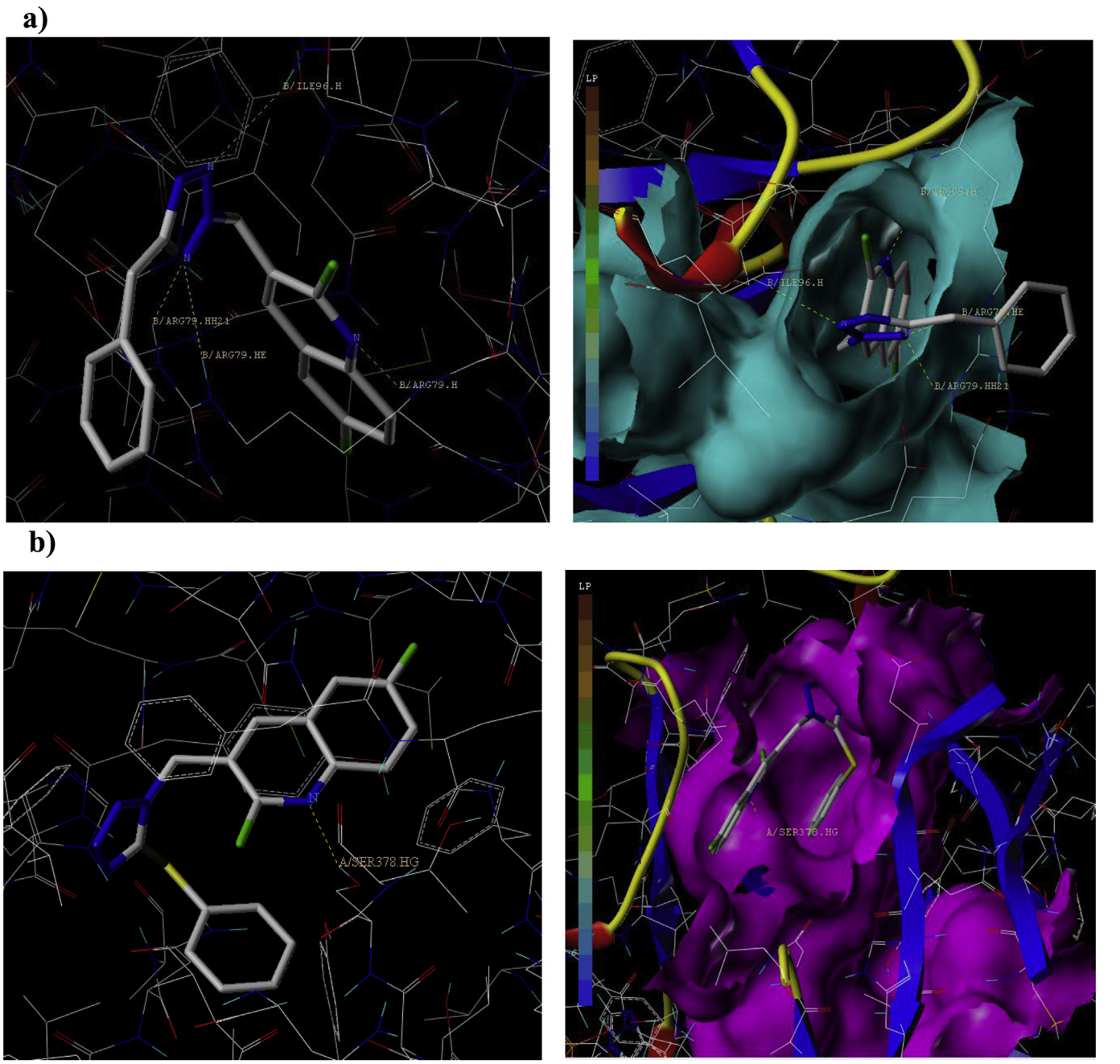

Fig. 7. (**a**) 3D binding model of compound **6k** docked into the active pocket of the enzyme DHFR, (**b**) 3D binding model of compound **7q** docked into the active pocket of the enzyme NMT.

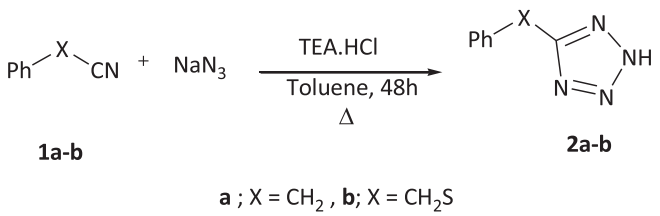

Scheme 1. Synthesis of compounds **2a-b**.

2.3. Single crystal X-ray analysis

The geometry of 2,5 and 1,5-regioisomers was studied by X-ray crystallographic studies. Molecular structure, numbering of atoms and the crystal packing of compound **6i** is depicted in Fig. 9. This compound crystallizes in a triclinic system with the P-1 space group and an asymmetric unit contains just one molecule. The lattice parameters a = 7.100 (4) Å, b = 10.339 (6) Å, c = 11.692 (7) Å, α = 66.611 (14) °, β = 77.985 (14) °, γ = 87.056 (16) °. The dihedral angle between quinoline rings with the tetrazole and benzene rings of the molecules are 77.53 (11) ° and 85.39 (12) respectively. In the structure, all bond lengths and angles are within normal ranges [57]. The crystal structure is stabilized by weak intermolecular C—H···N and C—H···O hydrogen bonds. The crystal packing is further stabilized by π—π and C—H … π interactions. The CIF file has been deposited with CCDC No. 1482262.

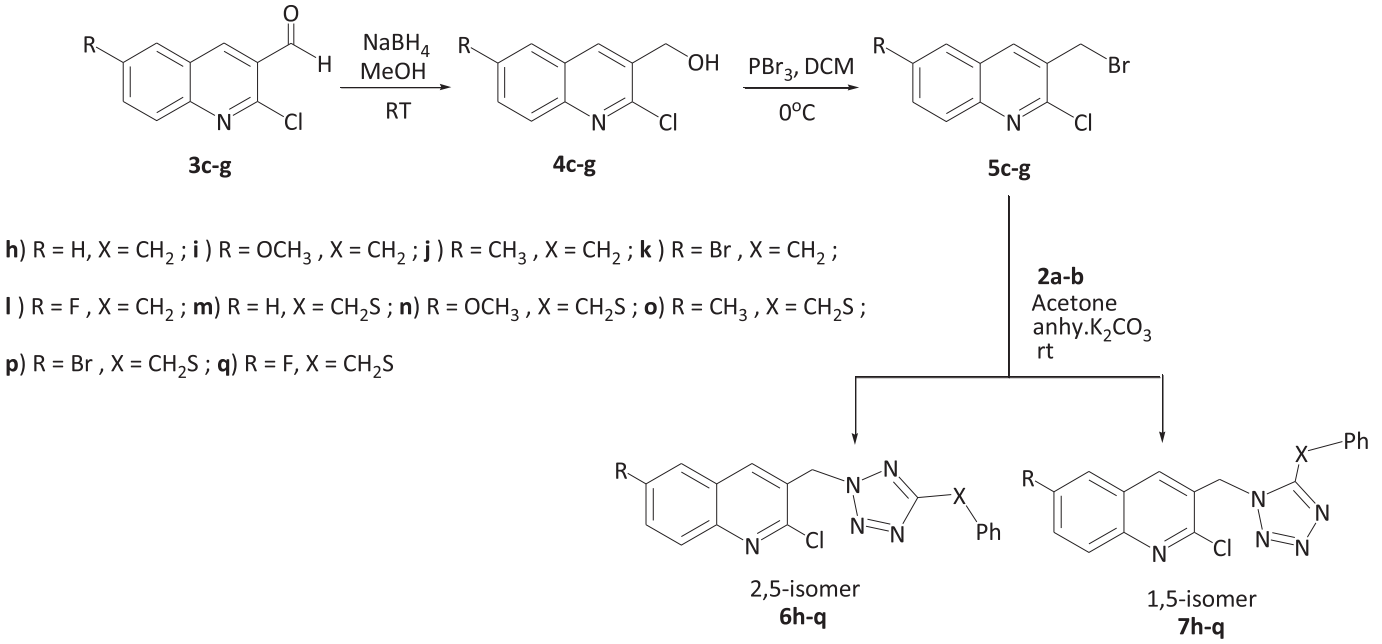

Scheme 2. Synthesis of title compounds **6h-q** and **7h-q**.

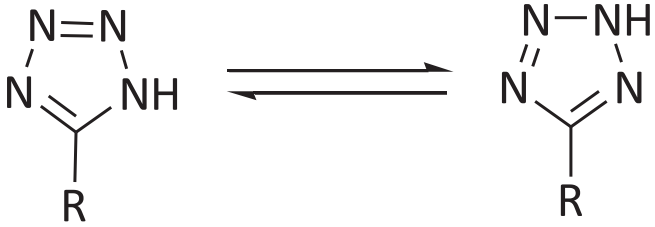

Fig. 8. 1*H* and 2*H*-Tautomers of 5-substituted tetrazoles.

The molecular structure, atom numbering and the crystal packing of compound **7h** is represented in Fig. 10. The compound **7h** crystallizes in a triclinic system with the P-1 space group and an asymmetric unit contains two crystallographically equivalent molecules. The lattice parameters are a = 8.6210 (2) Å, b = 12.4132 (3) Å, c = 16.1259 (4) Å, α = 74.2420 (10) °, β = 86.187 (2) °, γ = 81.483 (2) °. The dihedral angle between quinoline rings with the tetrazole and benzene rings of the molecules are 79.54 (8) ° & 3.13 (12) for one molecule and 74.22 (11) ° & 48.20 (11) respectively. In the structure, all bond lengths and angles are within normal ranges. The crystal structure is stabilized by other intermolecular C—H···N hydrogen bonds. In the crystal, inversion related C—H···N interactions generate an $R_2^2(8)$ ring pattern. The crystal packing

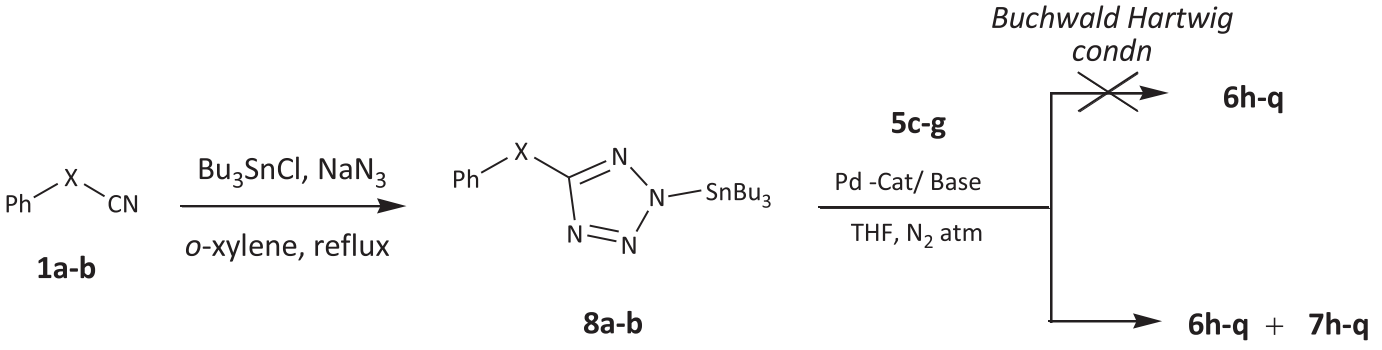

Scheme 3. Attempted synthetic route to get regioselective product **6h-q** by *Buchwald Hartwig* reaction.

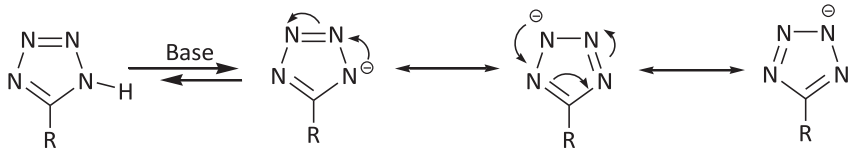

Scheme 4. Tautomerism in 5-substituted tetrazoles.

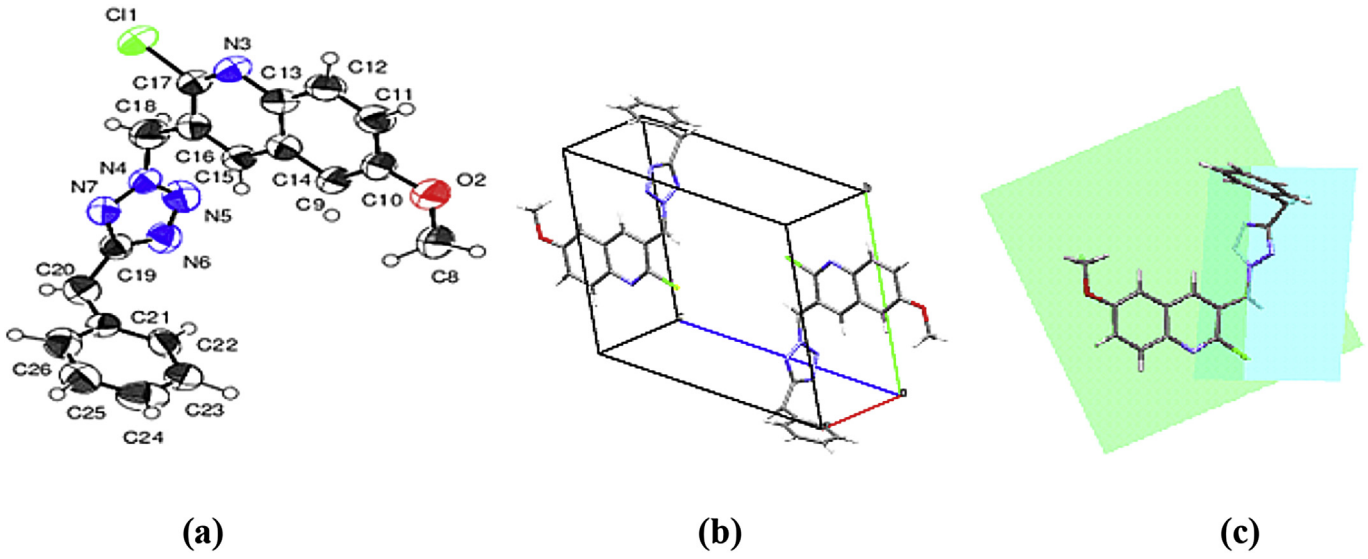

Fig. 9. (**a**) The ORTEP structure of compound **6i** (Displacement ellipsoids are drawn at the 50% probability level), (**b**) Packing diagram of compound **6i**, (**c**) Planes of the compound **6i**.

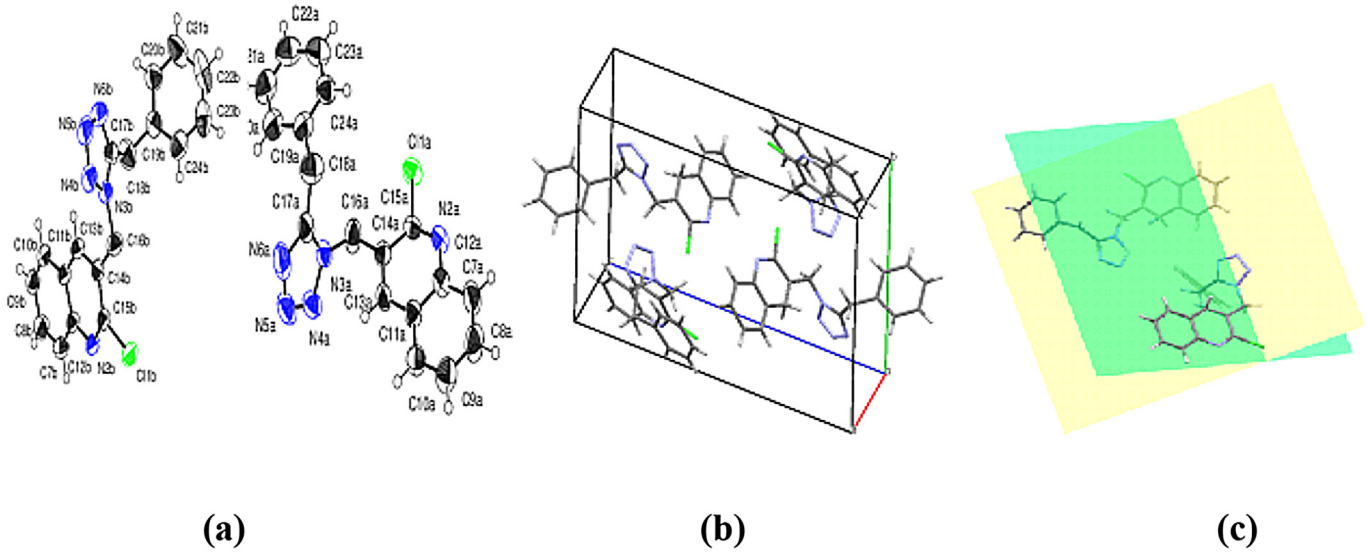

Fig. 10. (**a**) The ORTEP structure of compound **7h** (Displacement ellipsoids are drawn at the 50% probability level), (**b**) Packing diagram of compound **7h**, (**c**) Planes of the compound **7h**.

further stabilized by π–π and C—H … π interaction. The CIF file has also been deposited with CCDC No. 1482510.

2.4. Anticancer activity

The newly synthesized compounds were also subjected to *in vitro* anticancer screening in a single high dose (10^{-5} M) concentration against full 60 human cancer cell lines at the National Cancer Institute (NCI), USA under DTP drug therapeutics program. The output from the single dose screen is reported as a graph of mean growth percent of the treated cells and is available for analysis by the COMPARE program [58]. This allows detecting both growth inhibition values (between 0 and 100) and cytotoxicity values (less than 0). All the synthesized compounds **6h-q** and **7h-q** have been registered and 14 of them were selected for anticancer activity. The compounds **6h** (NSC: D-785704/1), **6i** (NSC: D-785706/1), **6k** (NSC: D-785708/1), **6l** (NSC: D-785710/1), **6m** (NSC: D-787573/1), **6o** (NSC: D-787575/1), **6q** (NSC: D-787577/1), **7h** (NSC: D-785705/1), **7i** (NSC: D-785707/1), **7k** (NSC: D-785709/1), **7l** (NSC: D-785711/1), **7m** (NSC: D-787574/1), **7o** (NSC: D-787576/1), **7q** (NSC: D-787578/1) have been screened for single high dose (10^{-5} M) concentration on all the 60 human cancer cell lines methodized into nine sub-panels derived from nine different human cancer types: leukemia, non-small cell lung, cancer, colon, CNS, melanoma, ovarian, renal, prostate and breast cancer cell lines.

Following are the percentage growth inhibition (GI %) of the treated cells at 10^{-5} M concentration of the compound **6h** (2,5-isomer without substitution, Table 2): Melanoma SK-MEL-5 (GI % 99.28), Ovarian Cancer OVCAR-4 (GI % 70.32), Breast Cancer MDA-MB-468 (GI % 88.92) and cytotoxicity effect against Renal Cancer UO-31 cell line. Compound **6i** (2,5-isomer with methoxy substitution, Table 2): Leukemia MOLT-4 (GI % 89.65), Non-Small Cell Lung Cancer EKVX (GI % 75.51), Colon Cancer COLO 205 (GI % 75.09), CNS Cancer SF-295 (GI % 62.61), Melanoma UACC-257 (GI % 73.55),

Table 2
Growth inhibition (GI %) in single dose assay (10^{-5}M) concentration for compound **6h** (NSC: D-785704/1) and **6i** (NSC: D-785706/1).

Panel/Cell line	**6h** Growth Inhibition (GI %)	**6i** Growth Inhibition (GI %)
Leukemia		
HL-60(TB)	12.11	43.42
K-562	44.81	67.10
MOLT-4	56.88	89.65
SR	63.02	77.09
Non-Small Cell Lung Cancer		
A549/ATCC	46.10	68.50
EKVX	63.86	75.51
NCI-H226	41.76	61.00
NCI-H23	54.45	67.46
NCI-H460	25.68	60.05
NCI-H522	57.89	61.95
Colon Cancer		
COLO 205	17.26	75.09
HCC-2998	18.68	40.99
HCT-116	64.93	70.81
HCT-15	35.00	63.53
HT29	28.45	72.60
KM12	33.68	63.52
SW-620	13.42	33.59
CNS Cancer		
SF-268	34.29	48.51
SF-295	52.44	62.61
SF-539	18.8	32.50
SNB-19	10.15	42.04
SNB-75	44.64	42.90
U251	23.74	46.77
Melanoma		
LOX IMVI	46.42	57.12
MALME-3M	34.40	65.62
M14	26.40	69.70
MDA-MB-435	34.69	70.71
SK-MEL-2	41.24	50.41
SK-MEL-28	15.32	52.55
SK-MEL-5	99.28	147.15(Cytotoxic)
UACC-257	46.37	73.55
UACC-62	48.28	64.87
Ovarian Cancer		
IGROV1	49.09	56.76
OVCAR-3	40.46	50.15
OVCAR-4	70.32	80.26
OVCAR-5	−4.25	17.18
OVCAR-8	28.39	59.53
NCI/ADR-RES	47.87	79.89
SK-OV-3	42.58	50.64
Renal Cancer		
786−0	27.12	52.54
ACHN	47.82	58.53
CAKI-1	59.51	56.07
RXF 393	16.07	39.83
SN12C	29.69	42.70
TK-10	39.08	65.07
UO-31	181.01(Cytotoxic)	85.26
Prostate Cancer		
DU-145	24.83	38.39
Breast Cancer		
MCF7	54.24	72.06
MDA-MB-231/ATCC	46.95	49.28
HS 578T	23.40	31.08
BT-549	61.06	79.66
T-47D	73.93	97.56
MDA-MB-468	88.92	70.08

Ovarian Cancer OVCAR-4 (GI % 80.26), Renal Cancer UO-31 (GI % 85.26), Prostate Cancer DU-145 (GI % 38.39), Breast Cancer T-47D (GI % 97.56) and has shown cytotoxicity effect against Melanoma SK-MEL-5 cell line. Rest of the compounds (**6k-m**, **6o**, **6q** and **7h-7q**) showed moderate GI% against all the cell lines.

2.5. Antifungal activity

Considering the interactions and binding modes of synthesized compounds with NMT and DHFR by docking studies, the *in vitro* antifungal activity was evaluated. The antifungal activity of synthesized compounds was tested against *A. fumigatus* and *C. albicans* strains using Fluconazole as reference by the Disc Diffusion method. The Zone of Inhibition (ZOI) and Minimum Inhibitory Concentrations (MIC) are summarized in Table 3. Antifungal activity with MIC$\leq$ 50 μg/ml was observed in all the derivatives. Drastic change was observed when compared with the regioisomers of the same derivative showing the affinity of molecule towards fungal strains. The derivatives having halo-substituents showed good activity when compared with other derivatives. Compounds **6k**, **6l**, **6p**, **7k**, **7l**, **7p** showed good activity at minimal concentrations, whereas compounds **6q** and **7q** (the 2,5- and 1,5-isomer with *fluoro* substituent at the 6th position) showed an excellent activity against *A. fumigatus* compared to *C. albicans*, at a low MIC value of 2.5 μg/ml. All other compounds showed moderate to good activity when compared to the standard.

Generally it was observed that halogens such as F and Br at the 6th position contributed to the *in vitro* results in case of antifungal activity, whereas H,OCH_3, CH_3 has less effects. Especially, fluorine at the 6th position is responsible for the increase in *in vitro* activity [59]. The increase in activity with respect to the substituents follows the sequence as, F > Br > $OCH_3 \geq CH_3$>H. In case of *in vitro* anticancer activity, we observed the change in order of sequence of activity as OCH_3>H > CH_3>Br > F. The significance of spatial determinators contributes little to the activity when attached to the acidic part, but when the length increases, it leads to substantial decrease in the activity [60]. Interestingly, *in vitro* antifungal activity revealed that the 1,5-regiosomer has shown more inhibition compared to 2,5-regioisomer indicating the regioselectivity of an enzyme.

3. Conclusions

A library of 2,5- and 1,5-regioisomers *viz*., 3-[(5-benzyl/benzyl thio-2*H*-tetrazol-2-yl) methyl]-2-chloro-6-substituted quinoline **6h-q** and 3-[(5-benzyl/benzyl thio-1*H*-tetrazol-1-yl) methyl]-2-chloro-6-substituted quinoline **7h-q** respectively have been synthesized and thoroughly characterized. Docking methods revealed that compounds **6h** and **6i** are covalent cross linker and an intercalator on the DNA helix structure of the protein structure owing to the *in vitro* results. Amongst 20 compounds, 14 compounds were screened at a single high dose (10^{-5} M) concentration. Out of these, compounds **6h** and **6i** have shown 40−99% growth inhibition of the tumor cells against various cell lines at 10^{-5} M concentration. Compounds **6h** and **6i** were also cytotoxic against Renal Cancer UO-31 and Melanoma SK-MEL-5 cell lines respectively. Docking into the active pocket of NMT and DHFR revealed that compounds (with *bromo* and *fluoro* substituents) **6k**, **6l**, **6p** and **7q** exhibited good binding mode into the amino acids, which are compatible with their *in vitro* screening results. Antifungal activity against *A. fumigatus* and *C. albicans*, showed inhibition at a minimal concentration of around (25−2.5) μg/ml. This revealed that compounds **6k** and **7q** are better inhibitors of DHFR and NMT respectively, hence showed excellent inhibition of fungal strains at minimal concentrations. It was interesting to note that, compounds **6h** and **6i** with good anticancer activity rather showed poor inhibition for fungal strain under investigation and the compounds **6k** and **7q** with potent antifungal property did not exhibit promising anticancer activity. These scaffolds with potent pharmacological property may be considered to be lead compounds for the development of potent anticancer and antifungal agents.

Table 3
In vitro antifungal activities of **6h-q** and **7h-q** expressed in ZOI (mm) and MIC (μg/ml).

Entry No.		ZOI (mm)	*C. albicans* MIC (μg/ml)	ZOI (mm)	*A. fumigatus* MIC (μg/ml)
6h		10	25	16	50
6i		16	10	20	25
6j		12	25	12	25
6k		10	10	13	10
6l	→ 2,5-Regioisomers	12	25	15	25
6m		10	10	15	25
6n		16	25	20	10
6o		12	10	18	25
6p		18	25	15	5
6q		18	50	13	2.5
7h		10	25	14	50
7i		15	25	20	25
7j		10	25	10	25
7k		16	10	13	10
7l	→ 1,5-Regioisomers	13	25	10	10
7m		12	10	16	25
7n		18	25	18	10
7o		12	10	16	25
7p		12	25	20	5
7q		13	50	14	2.5
Standard		24	30	26	30

4. Experimental section

4.1. General

All AR grade common reagents and solvents were obtained from Sigma Aldrich, SD fine chemicals and Alfa Aesar and used without further purification. Thin layer chromatography (TLC) was performed on Merck Silica Gel 60 F_{254} and visualized under UV light chamber. Melting points were determined in open capillary tubes and are uncorrected. Column chromatography was carried out using silica gel (Silica Gel 60–120 mesh, 120–250 μm). ^{1}H (400 MHz) and ^{13}C (100 MHz) NMR spectra were recorded on Bruker AV-400 and JEOL JNM-ECX500II spectrometer respectively using DMSO-d_6. Chemical shifts (δ) were reported as parts per million (ppm) relative to tetramethylsilane (TMS) as an internal standard. Mass spectra were recorded using a Finnegan MAT (Model MAT 8200) spectrometer. Elemental analyses for C, H and N were performed using a Heraeus CHN rapid analyzer. Single Crystal X-ray analyses were carried out using Bruker SMART CCD area-detector diffractometer with monochromatic Mo *Kα* radiation at room temperature. The crystalline state of a crystal is characterized by a long range, well defined three dimensional orders.

4.2. Synthetic procedures and spectral data

4.2.1. General procedure for the synthesis of 5-(benzyl/benzylthio)-2H-tetrazole (**2a-b**)

A mixture of benzyl cyanide (0.003 mol), NaN_3 (0.0134 mol) and triethylamine hydrochloride (TEA.HCl) (0.013 mol) in toulene was heated to 110–115 °C for 48 h with stirring. The reaction mixture was cooled to room temperature and stirred for 30 min at RT. The product was extracted with water (15 ml) and NaOH solution (5%, 2 ml). To the aqueous layer which is basic in condition, dilute hydrochloric acid was added drop wise to get tetrazole product. After filtration the product was dried under reduced pressure to get a crude product which was recyrstallised from acetone to get the compound **2a-b**.

4.2.2. General procedure for the synthesis of 2-chloroquinolin-3-carbaldehyde (**3c-g**)

Vilsmeir-Haack adduct was prepared by adding phosphorous oxychloride (0.35 mol) drop wise to the cold solution of DMF (0.125 mol) with constant stirring. To this adduct, substituted acetanilide (0.05 mol) was added slowly and stirred well for 15–20 min. The mixture was then refluxed for 16 h at 70–80 °C. After completion of the reaction, the contents were then poured into ice water and stirred for 30 min. The 2-chloroquinoline-3-carbaldehyde **3c-g** was precipitated which was filtered and washed well with water. Dried and recrystallised from ethyl acetate.

4.2.3. General procedure for the synthesis of (2-chloroquinolin-3-yl) methanol (**4c-g**)

To the well stirred mixture of 2-chloroquinoline-3-carbaldehyde **3c-g** (0.01 mol) in methanol (10 ml), $NaBH_4$ (0.01 mol) was added in small portions, and the mixture was stirred at room temperature for 15–20 min. The completion of the reaction was monitored by TLC and the reaction mixture was concentrated under vacuum. The mixture was poured into ice cold water and the (2-chloroquinolin-3-yl) methanol **4c-g** separated as solid was filtered off and recrystallised from ethyl acetate.

4.2.4. Synthesis of 3-(bromomethyl)-2-chloro-6-substituted quinoline (**5c-g**)

(2-Chloroquinolin-3-yl) methanol (0.01 mol) was dissolved in DCM (10–15 ml) at 5 °C and stirred well. After 10–15 min, PBr_3

(6 mmol) was added drop wise and stirred at room temperature for 1 h. After completion of the reaction, DCM was removed under vacuum and the mixture was poured into ice and neutralized by adding a saturated solution of $NaHCO_3$. The precipitate was filtered and dried.

*4.2.5. General procedure for the synthesis of 5-(benzyl/benzylthio)-2-(tributylstannyl)-2H-tetrazole (**8a-b**)*

Tributyltin chloride (2.5 mol) and NaN_3 (2.5 mol) were charged into a solution of appropriate nitrile (1.0 mol) taken in *o*-xylene (20 ml). The reaction mixture was stirred at reflux for stipulated time of 15 h. After completion of the reaction, the solvent was evaporated to get the oily compound **8a-b**.

*4.2.6. Preparation of 3-[(5-benzy/benzylthio-2H-tetrazol-2-yl) methyl]-2-chloro-6-substituted quinoline (**6h-q**) and 3-[(5-benzyl/ benzylthio-1H-tetrazol-1-yl)methyl]-2-chloro-6-substituted quinoline (**7h-q**)*

Mixture of 5-(benzyl/benzylthio)-2*H*-tetrazole (**2a-b**) (0.01mol) and 3-(bromomethyl)-2-chloro-6-substituted quinoline (**5c-g**) (0.01mol) and anhydrous potassium carbonate (0.02 mol) in dry acetone was stirred at room temperature until the completion of reaction by TLC, hexane: ethyl acetate (7:3). The reaction mixture was filtered, washed with acetone and the filtrate was evaporated to dryness to get regioisomers which were further separated by column chromatography using hexane: ethyl acetate (30%) as an eluent.

*4.2.6.1. 3-[(5-Benzyl-2H-tetrazol-2-yl)methyl]-2-chloroquinoline **6h**.* White solid; Yield: 85%; m.p. 94–96 °C; IR (KBr, cm^{-1}): 3034 (C-H), 1619 (C═N), 1591 (C═C). ^{1}H NMR (400 MHz, DMSO-d_6, δ ppm): 8.05 (1H, d, J_{78} = 8.8 Hz, "H_8″ ArH), 7.97 (1H, d, J_{48} = 0.8 Hz, "H_4″ ArH), 7.86 (1H, d, J_{56} = 8.4 Hz, "H_5″ ArH), 7.71 (1H, dd, J_{67} = 7.2 Hz and J_{78} = 8.4 Hz, "H_7″ ArH), 7.69 (1H, dd, J_{67} = 7.6 Hz and J_{65} = 8.4 Hz, "H_6″ ArH), 7.19–7.30 (5H, m, ArH), 6.13 (2H, s, N-CH_2), 4.22 (2H, s, CH_2 of benzyl). ^{13}C NMR (100 MHz, DMSO-d_6, δ ppm): 165.22, 149.32, 146.74, 140.97, 136.86, 131.60, 128.56, 128.25, 127.95, 127.85, 127.62, 127.46, 126.63, 126.58, 53.74, 30.73. Calcd Mass 335.79 MS (*m*/*z*): 337.09 (M^{+2}), 335.09 (M^+). Anal. Calcd for $C_{18}H_{14}N_5Cl$: C, 64.38; H, 4.20; N, 20.86. Found: C, 64.49; H, 4.28; N, 20.89.

*4.2.6.2. 3-[(5-Benzyl-2H-tetrazol-2-yl)methyl]-2-chloro-6-methoxyquinoline **6i**.* White solid; Yield: 91%; m.p. 96–98 °C; IR (KBr, cm^{-1}): 3056 (C-H), 1619 (C═N), 1595 (C═C). ^{1}H NMR (400 MHz, DMSO-d_6, δ ppm): 8.36 (1H, d, J_{78} = 8.6 Hz, "H_8″ ArH), 7.87 (1H, d, J_{48} = 0.8 Hz, "H_4″ ArH), 7.50 (1H, d, J_{57} = 1.6 Hz, "H_5″ArH), 7.47 (1H, dd, J_{57} = 1.6 Hz and J_{78} = 8.6 Hz, "H_7″ ArH), 7.19–7.30 (5H, m, ArH), 6.11 (2H, s, N-CH_2), 4.22 (2H, s, CH_2 of benzyl), 3.89 (3H, s, CH_3). ^{13}C NMR (100 MHz, DMSO-d_6, δ ppm): 165.84, 158.67, 147.03, 143.25, 140.05, 137.48, 129.63, 129.19, 129.07, 128.59, 127.21, 126.43, 124.48, 106.59, 56.28, 54.31, 31.37. Calcd Mass 365.82 MS (*m*/*z*): 367.10 (M^{+2}), 365.10 (M^+). Anal. Calcd for $C_{19}H_{16}N_5OCl$: C, 62.38; H, 4.41; N, 19.14. Found: C, 62.43; H, 4.43; N, 19.10.

*4.2.6.3. 3-[(5-Benzyl-2H-tetrazol-2-yl)methyl]-2-chloro-6-methylquinoline **6j**.* Off White solid; Yield: 89%; m.p. 78–80 °C; IR (KBr, cm^{-1}): 3061 (C-H), 1617 (C═N), 1565 (C═C). ^{1}H NMR (400 MHz, DMSO-d_6, δ ppm): 8.38 (1H, d, J_{78} = 8.8 Hz, "H_8″ ArH), 7.84 (1H, d, J_{48} = 0.8 Hz, "H_4″ ArH), 7.50 (1H, d, J_{57} = 1.6 Hz, "H_5″ArH), 7.49 (1H, dd, J_{57} = 1.6 Hz and J_{78} = 8.8 Hz, "H_7″ ArH), 7.11–7.32 (5H, m, ArH), 6.13 (2H, s, N-CH_2), 4.22 (2H, s, CH_2 of benzyl), 2.32 (3H, s, CH_3). ^{13}C NMR (100 MHz, DMSO-d_6, δ ppm): 165.78, 159.11, 147.32, 136.43, 136.39, 135.60, 131.56, 129.78, 129.58, 129.13, 129.04, 128.64, 127.42, 126.58, 125.34, 54.6, 31.33, 23.67. Calcd Mass 349.82 MS (*m*/*z*): 351.11 (M^{+2}), 349.11 (M^+). Anal. Calcd for $C_{19}H_{16}N_5Cl$: C, 65.24; H, 4.61; N, 20.02. Found: C, 65.20; H, 4.58; N, 20.11.

*4.2.6.4. 3-[(5-Benzyl-2H-tetrazol-2-yl)methyl]-6-bromo-2-chloroquinoline **6k**.* Pale yellow solid; Yield: 85%; m.p. 104–106 °C; IR (KBr, cm^{-1}): 3067 (C-H), 1595 (C═N), 1556 (C═C). ^{1}H NMR (400 MHz, DMSO-d_6, δ ppm): 8.42 (1H, d, J_{78} = 8.6 Hz, "H_8″ ArH), 7.97 (1H, d, J_{48} = 1.2 Hz, "H_4″ ArH), 7.85 (1H, d, J_{57} = 1.4 Hz, "H_5″ ArH), 7.61 (1H, dd, J_{57} = 1.4 Hz and J_{78} = 8.4 Hz, "H_7″ ArH), 7.10–7.31 (5H, m, ArH), 6.10 (2H, s, N-CH_2), 4.21 (2H, s, CH_2 of benzyl). ^{13}C NMR (100 MHz, DMSO-d_6, δ ppm): 165.32, 149.66, 147.62, 136.52, 136.24, 133.32, 131.48, 130.7, 129.69, 129.51, 128.87, 128.45, 127.89, 118.78, 56.43, 31.43. Calcd Mass 414.69 MS (*m*/*z*): 417.12 (M^{+4}), 415.11 (M^{+2}), 413.10 (M^+). Anal. Calcd for $C_{18}H_{13}N_5BrCl$: C, 52.13; H, 3.16; N, 16.89. Found: C, 52.10; H, 3.13; N, 16.85.

*4.2.6.5. 3-[(5-Benzyl-2H-tetrazol-2-yl)methyl]-2-chloro-6-fluoroquinoline **6l**.* Pale yellow solid; Yield: 87%; m.p. 80–82 °C; IR (KBr, cm^{-1}): 3058 (C-H), 1596 (C═N), 1567 (C═C). ^{1}H NMR (400 MHz, DMSO-d_6, δ ppm): 8.51 (1H, d, J_{78} = 8.4 Hz, "H_8″ ArH), 8.45 (1H, d, J_{48} = 0.8 Hz, "H_4″ ArH), 7.92 (1H, d, J_{57} = 1.4 Hz, "H_5″ ArH), 7.79 (1H, dd, J_{57} = 1.4 Hz and J_{78} = 8.6 Hz, "H_7″ ArH), 7.19–7.28 (5H, m, ArH), 6.14 (2H, s, N-CH_2), 4.22 (2H, s, CH_2 of benzyl). ^{13}C NMR (100 MHz, DMSO-d_6, δ ppm): 165.39, 158.34, 154.65, 140.25, 139.74, 136.84, 136.33, 130.68, 130.60, 128.59, 128.45, 126.60, 121.73, 111.72, 55.34, 30.73. Calcd Mass 353.78 MS (*m*/*z*): 355.08 (M^{+2}), 353.08(M^+). Anal. Calcd for $C_{18}H_{13}N_5FCl$: C, 61.11; H, 3.70; N, 19.80. Found: C, 61.13; H, 3.68; N, 19.82.

*4.2.6.6. 3-[(5-(Benzylthio)-2H-tetrazol-2-yl)methyl]-2-chloroquinoline **6m**.* White solid; Yield: 82%; m.p. 102–104 °C; IR (KBr, cm^{-1}): 3067 (C-H), 1615 (C═N), 1594 (C═C), 690 (C-S). ^{1}H NMR (400 MHz, DMSO-d_6, δ ppm): 8.59 (1H, d, J_{78} = 8.6 Hz, "H_8″ ArH), 8.54 (1H, d, J_{48} = 1.6 Hz, "H_4″ ArH), 8.09 (1H, d, J_{56} = 8.2 Hz, "H_5″ ArH), 7.99 (1H, dd, J_{67} = 6.8 Hz and J_{78} = 8.6 Hz, "H_7″ ArH), 7.86 (1H, dd, J_{67} = 6.8 Hz and J_{65} = 8.4 Hz, "H_6″ ArH), 7.15–7.73 (5H, m, ArH), 6.11 (2H, s, N-CH_2), 4.36 (2H, s, CH_2 of benzyl). ^{13}C NMR (100 MHz, DMSO-d_6, δ ppm): 162.86, 149.38, 147.45, 142.63, 141.30, 136.99, 131.76, 128.86, 128.39, 128.27, 127.93, 127.70, 127.65, 127.34, 55.97, 34.13. Calcd Mass 369.87 MS (*m*/*z*): 371.08 (M^{+2}), 369.08(M^+). Anal. Calcd for $C_{18}H_{14}N_5SCl$: C, 57.71; H, 3.42; N, 19.79. Found: C, 57.69; H, 3.45; N, 19.81.

*4.2.6.7. 3-[(5-(Benzylthio)-2H-tetrazol-2-yl)methyl]-2-chloro-6-methoxyquinoline **6n**.* White solid; Yield: 78%; m.p. 96–98 °C; IR (KBr, cm^{-1}): 3064 (C-H), 1618 (C═N), 1599 (C═C), 710 (C-S). ^{1}H NMR (400 MHz, DMSO-d_6, δ ppm): 8.36 (1H, d, J_{78} = 8.8 Hz, "H_8″ ArH), 7.87 (1H, d, J_{48} = 1.2 Hz, "H_4″ ArH), 7.49 (1H, d, J_{57} = 1.4 Hz, "H_5″ ArH), 7.47 (1H, dd, J_{57} = 1.4 Hz and J_{78} = 8.8 Hz, "H_7″ ArH), 7.14–7.65 (5H, m, ArH), 6.12 (2H, s, N-CH_2), 4.32 (2H, s, CH_2 of benzyl), 3.88 (3H, s, CH_3). ^{13}C NMR (100 MHz, DMSO-d_6, δ ppm): 165.78, 158.61, 146.88, 143.20, 139.64, 137.48, 129.59, 129.10, 129.01, 128.33, 127.21, 126.21, 124.56, 105.51, 57.45, 54.28, 34.32. Calcd Mass 397.88 MS (*m*/*z*): 399.07 (M^{+2}), 397.08(M^+). Anal. Calcd for $C_{19}H_{16}N_5OSCl$: C, 56.32; H, 3.68; N, 18.24. Found: C, 56.30; H, 3.61; N, 18.21.

*4.2.6.8. 3-[(5-(Benzylthio)-2H-tetrazol-2-yl)methyl]-2-chloro-6-methylquinoline **6o**.* Off white solid; Yield: 84%; m.p. 106–108 °C; IR (KBr, cm^{-1}): 3054 (C-H), 1598 (C═N), 1575 (C═C), 708 (C-S). ^{1}H NMR (400 MHz, DMSO-d_6, δ ppm): 8.39 (1H, d, J_{78} = 8.6 Hz, "H_8″ ArH), 7.85 (1H, d, J_{48} = 0.8 Hz, "H_4″ ArH), 7.49 (1H, d, J_{57} = 1.6 Hz, "H_5″ ArH), 7.49 (1H, dd, J_{57} = 1.59 Hz and J_{78} = 8.6 Hz, "H_7″ ArH),

7.13–7.62 (5H, m, ArH), 6.13 (2H, s, N-CH_2), 4.15 (2H, s, CH_2 of benzyl), 2.32 (3H, s, CH_3). ^{13}C NMR (100 MHz, DMSO-d_6, δ ppm): 165.64, 159.16, 147.34, 136.54, 136.21, 135.34, 131.45, 129.76, 129.55, 129.08, 129.03, 128.71, 126.55, 125.41, 54.75, 34.12, 23.58. Calcd Mass 381.88 MS (*m*/*z*): 383.08 (M^{+2}), 381.08 (M^{+}). Anal. Calcd for $C_{19}H_{16}N_5SCl$: C, 58.77; H, 3.84; N, 19.04. Found: C, 58.74; H, 3.87; N, 19.02.

4.2.6.9. 3-[(5-(Benzylthio)-2H-tetrazol-2-yl)methyl]-6-bromo-2-chloroquinoline ***6p***. Yellow solid; Yield: 80%; m.p. 108–110 °C; IR (KBr, cm^{-1}): 3069 (C-H), 1614 (C═N), 1596 (C═C), 717 (C-S). ^{1}H NMR (400 MHz, DMSO-d_6, δ ppm): 8.52 (1H, d, J_{78} = 8.6 Hz, "H_8″ ArH), 7.95 (1H, d, J_{48} = 1.2 Hz, "H_4″ ArH), 7.89 (1H, d, J_{57} = 1.6 Hz, "H_5″ ArH), 7.63 (1H, dd, J_{57} = 1.6 Hz and J_{78} = 8.6 Hz, "H_7″ ArH), 7.14–7.57 (5H, m, ArH), 6.12 (2H, s, N-CH_2), 4.11 (2H, s, CH_2 of benzyl). ^{13}C NMR (100 MHz, DMSO-d_6, δ ppm): 165.29, 149.54, 147.87, 136.48, 136.21, 133.30, 131.42, 130.54, 129.76, 129.48, 128.92, 128.73, 127.76, 117.76, 57.43, 34.13. Calcd Mass 446.75 MS (*m*/*z*): 448.97 (M^{+4}), 446.97 (M^{+2}), 444.98 (M). Anal. Calcd for $C_{18}H_{13}N_5SBrCl$: C, 47.19; H, 2.56; N, 16.18. Found: C, 47.21; H, 2.58; N, 16.20.

4.2.6.10. 3-[(5-(Benzylthio)-2H-tetrazol-2-yl)methyl]-2-chloro-6-fluoroquinoline ***6q***. Pale yellow solid; Yield: 88%; m.p. 112–114 °C; IR (KBr, cm^{-1}): 3078 (C-H), 1612 (C═N), 1574 (C═C), 721 (C-S). ^{1}H NMR (400 MHz, DMSO-d_6, δ ppm): 8.55 (1H, d, J_{78} = 8.4 Hz, "H_8″ ArH), 8.38 (1H, d, J_{48} = 0.8 Hz, "H_4″ ArH), 7.90 (1H, d, J_{57} = 1.4 Hz, "H_5″ ArH), 7.75 (1H, dd, J_{57} = 1.4 Hz and J_{78} = 8.4 Hz, "H_7″ ArH), 7.20–7.68 (5H, m, ArH), 6.152 (2H, s, N-CH_2), 4.08 (2H, s, CH_2 of benzyl). ^{13}C NMR (100 MHz, DMSO-d_6, δ ppm): 165.43, 149.31, 147.81, 140.21, 139.71, 136.78, 136.48, 130.64, 130.43, 128.61, 128.39, 126.54, 121.86, 111.69, 55.48, 34.18. Calcd Mass 385.85 MS (*m*/*z*): 387.05 (M^{+2}), 385.06 (M^{+}). Anal. Calcd for $C_{18}H_{13}N_5SFCl$: C, 54.91; H, 2.98; N, 18.84. Found: C, 54.89; H, 2.95; N, 18.86.

4.2.6.11. 3-[(5-Benzyl-1H-tetrazol-1-yl)methyl]-2-chloroquinoline ***7h***. White solid; Yield: 86%, m.p. 120–122 °C; IR (KBr, cm^{-1}): 3048 (C-H), 1628 (C═N), 1594 (C═C). ^{1}H NMR (400 MHz, DMSO-d_6, δ ppm): 8.02 (1H, d, J_{78} = 8.8 Hz, "H_8″ ArH), 7.93 (1H, d, J_{48} = 0.8 Hz, "H_4″ ArH), 7.84 (1H, d, J_{56} = 8.4 Hz, "H_5″ ArH), 7.80 (1H, dd, J_{67} = 7.4 Hz and J_{78} = 8.8 Hz, "H_7″ ArH), 7.64 (1H, dd, J_{67} = 7.6 Hz and J_{65} = 8.4 Hz, "H_6″ ArH), 7.05–7.22 (5H, m, ArH), 5.86 (2H, s, N-CH_2), 4.45 (2H, s, CH_2 of benzyl). ^{13}C NMR (100 MHz, DMSO-d_6, δ ppm): 153.48, 147.82, 136.76, 136.34, 131.68, 128.88, 128.54, 128.21, 127.98, 127.74, 127.49, 127.11, 126.63, 126.22, 55.34, 28.34. Calcd Mass 335.79 MS (*m*/*z*): 337.09 (M^{+2}), 335.09(M^{+}). Anal. Calcd for $C_{18}H_{14}N_5Cl$: C, 64.38; H, 4.20; N, 20.86. Found: C, 64.35; H, 4.22; N, 20.84.

4.2.6.12. 3-[(5-Benzyl-1H-tetrazol-1-yl)methyl]-2-chloro-6-methoxyquinoline ***7i***. White solid; Yield: 78%, m.p. 156–158 °C; IR (KBr, cm^{-1}): 3035 (C-H), 1623 (C═N), 1598 (C═C). ^{1}H NMR (400 MHz, DMSO-d_6, δ ppm): 8.21 (1H, d, J_{78} = 8.6 Hz, "H_8″ ArH), 7.70 (1H, d, J_{48} = 0.8 Hz, "H_4″ ArH), 7.44 (1H, d, J_{57} = 1.6 Hz, "H_5″ ArH), 7.42 (1H, dd, J_{57} = 1.6 Hz and J_{78} = 8.6 Hz, "H_7″ ArH), 7.06–7.31 (5H, m, ArH), 5.84 (2H, s, N-CH_2), 4.44 (2H, s, CH_2 of benzyl), 3.86 (3H, s, CH_3). ^{13}C NMR (100 MHz, DMSO-d_6, δ ppm): 157.94, 154.83, 145.50, 142.35, 137.18, 134.57, 128.89, 128.74, 128.52, 127.93, 126.88, 126.29, 123.59, 105.98, 55.69, 47.73, 28.17. Calcd Mass 365.82 MS (*m*/*z*): 367.10 (M^{+2}), 365.10 (M^{+}). Anal. Calcd for $C_{19}H_{16}N_5OCl$: C, 62.38; H, 4.41; N, 19.14. Found: C, 62.40; H, 4.45; N, 19.16.

4.2.6.13. 3-[(5-Benzyl-1H-tetrazol-1-yl)methyl]-2-chloro-6-methylquinoline ***7j***. Off white solid; Yield: 76%, m.p. 128–130 °C; IR (KBr, cm^{-1}): 3036 (C-H), 1599 (C═N), 1564 (C═C). ^{1}H NMR (400 MHz, DMSO-d_6, δ ppm): 8.05 (1H, d, J_{78} = 8.8 Hz, "H_8″ ArH), 7.86 (1H, d, J_{48} = 0.8 Hz, "H_4″ ArH), 7.53 (1H, d, J_{57} = 1.6 Hz, "H_5″ ArH), 7.34 (1H, dd, J_{57} = 1.6 Hz and J_{78} = 8.8 Hz, "H_7″ ArH), 7.03–7.33 (5H, m, ArH), 5.76 (2H, s, N-CH_2), 4.38 (2H, s, CH_2 of benzyl), 2.30 (3H, s, CH_3). ^{13}C NMR (100 MHz, DMSO-d_6, δ ppm): 154.72, 149.44, 147.64, 136.89, 136.65, 136.33, 131.46, 128.94, 128.72, 127.88, 127.56, 127.45, 127.38, 126.65, 55.48, 28.32, 23.58. Calcd Mass 349.82 MS (*m*/*z*): 351.11 (M^{+2}), 349.11 (M^{+}). Anal. Calcd for $C_{19}H_{16}N_5Cl$: C, 65.24; H, 4.61; N, 20.02. Found: C, 65.22; H, 4.64; N, 20.00.

4.2.6.14. 3-[(5-Benzyl-1H-tetrazol-1-yl) methyl]-6-bromo-2-chloroquinoline ***7k***. Pale yellow solid; Yield: 82%, m.p. 130–132 °C; IR (KBr, cm^{-1}): 3062 (C-H), 1613 (C═N), 1591 (C═C). ^{1}H NMR (400 MHz, DMSO-d_6, δ ppm): 8.47 (1H, d, J_{78} = 8.59 Hz, "H_8″ ArH), 8.20 (1H, d, J_{48} = 0.8 Hz, "H_4″ ArH), 7.88 (1H, d, J_{57} = 1.2 Hz, "H_5″ ArH), 7.62 (1H, dd, J_{57} = 1.4 Hz and J_{78} = 8.4 Hz, "H_7″ ArH), 7.11–7.30 (5H, m, ArH), 5.89 (2H, s, N-CH_2), 4.19 (2H, s, CH_2 of benzyl). ^{13}C NMR (100 MHz, DMSO-d_6, δ ppm): 154.77, 149.67, 147.62, 136.91, 136.24, 133.41, 131.48, 129.96, 129.82, 128.97, 128.71, 128.45, 127.89, 118.78, 56.65, 31.38. Calcd Mass 414.69 MS (*m*/*z*): 417.00 (M^{+4}), 415.00 (M^{+2}), 413.00 (M^{+}). Anal. Calcd for $C_{18}H_{13}N_5BrCl$: C, 52.13; H, 3.16; N, 16.89. Found: C, 52.11; H, 3.10; N, 16.87.

4.2.6.15. 3-[(5-Benzyl-1H-tetrazol-1-yl)methyl]-2-chloro-6-fluoroquinoline ***7l***. Pale yellow solid; Yield: 74%, m.p. 100–102 °C; IR (KBr, cm^{-1}): 3062 (C-H), 1593 (C═N), 1565 (C═C). ^{1}H NMR (400 MHz, DMSO-d_6, δ ppm): 8.80 (1H, d, J_{78} = 8.6 Hz, "H_8″ ArH), 8.19 (1H, d, J_{48} = 0.8 Hz, "H_4″ ArH), 7.82 (1H, d, J_{57} = 1.4 Hz, "H_5″ ArH), 7.71 (1H, dd, J_{57} = 1.4 Hz and J_{78} = 8.6 Hz, "H_7″ ArH), 7.10–7.37 (5H, m, ArH), 5.82 (2H, s, N-CH_2), 4.44 (2H, s, CH_2 of benzyl). ^{13}C NMR (100 MHz, DMSO-d_6, δ ppm): 161.32, 158.95, 154.81, 144.19, 137.86, 137.26, 130.49, 130.32, 128.84, 128.67, 127.06, 126.78, 121.07, 111.65, 49.44, 28.26. Calcd Mass 353.78 MS (*m*/*z*): 355.08 (M^{+2}), 353.08 (M^{+}). Anal. Calcd for $C_{18}H_{13}N_5FCl$: C, 61.11; H, 3.70; N, 19.80. Found: C, 61.15; H, 3.67; N, 19.79.

4.2.6.16. 3-[(5-(Benzylthio)-1H-tetrazol-1-yl)methyl]-2-chloroquinoline ***7m***. White solid; Yield: 79%, m.p. 128–130 °C; IR (KBr, cm^{-1}): 3069 (C- H), 1625 (C═N), 1591 (C═C), 717 (C-S). ^{1}H NMR (400 MHz, DMSO-d_6, δ ppm): 8.22 (1H, d, J_{78} = 8.6 Hz, "H_8″ ArH), 8.00 (1H, d, J_{48} = 1.6 Hz, "H_4″ ArH), 7.94 (1H, d, J_{56} = 8.2 Hz, "H_5″ ArH), 7.82 (1H, dd, J_{67} = 6.8 Hz and J_{78} = 8.6 Hz, "H_7″ ArH), 7.66 (1H, dd, J_{67} = 6.8 Hz and J_{65} = 8.4 Hz, "H_6″ ArH), 7.18–7.33 (5H, m, ArH), 5.66 (2H, s, N-CH_2), 4.52 (2H, s, CH_2 of benzyl). ^{13}C NMR (100 MHz, DMSO-d_6, δ ppm): 153.80, 148.83, 147.28, 139.61, 136.41, 131.61, 128.97, 128.94, 128.48, 128.34, 127.98, 127.88, 127.72, 127.58, 50.07, 36.88. Calcd Mass 367.86 MS (*m*/*z*): 369.06 (M^{+2}), 367.07 (M^{+}). Anal. Calcd for $C_{18}H_{14}N_5SCl$: C, 57.71; H, 3.42; N, 19.79. Found: C, 57.69; H, 3.40; N, 19.77.

4.2.6.17. 3-[(5-(Benzylthio)-1H-tetrazol-1-yl)methyl]-2-chloro-6-methoxyquinoline ***7n***. White solid; Yield: 89%, m.p. 134–136 °C; IR (KBr, cm^{-1}): 3071 (C-H), 1621 (C═N), 1589 (C═C), 712 (C-S). ^{1}H NMR (400 MHz, DMSO-d_6, δ ppm): 8.37 (1H, d, J_{78} = 8.8 Hz, "H_8″ ArH), 7.88 (1H, d, J_{48} = 1.2 Hz, "H_4″ ArH), 7.51 (1H, d, J_{57} = 1.4 Hz, "H_5″ ArH), 7.49 (1H, dd, J_{57} = 1.4 Hz and J_{78} = 8.8 Hz, "H_7″ ArH), 7.16–7.41 (5H, m, ArH), 6.11 (2H, s, N-CH_2), 4.48 (2H, s, CH_2 of benzyl), 3.82 (3H, s, CH_3). ^{13}C NMR (100 MHz, DMSO-d_6, δ ppm): 158.61, 154.71, 147.88, 145.64, 142.35, 137.48, 130.10, 129.89, 129.81, 129.37, 129.18, 127.21, 123.56, 105.63, 56.97, 54.66, 36.85. Calcd Mass 397.88 MS (*m*/*z*): 399.07 (M^{+2}), 397.08 (M^{+}). Anal. Calcd for $C_{19}H_{16}N_5OSCl$: C, 56.32; H, 3.68; N, 18.24. Found: C, 56.29; H, 3.65;

N, 18.25.

4.2.6.18. 3-[(5-(Benzylthio)-1H-tetrazol-1-yl)methyl]-2-chloro-6-methylquinoline ***7o***. Off white solid; Yield: 76%, m.p. 128–130 °C; IR (KBr, cm^{-1}): 3056 (C-H), 1594 (C═N), 1572 (C═C), 711 (C- S). ^1H NMR (400 MHz, DMSO-d_6, δ ppm): 8.42 (1H, d, J_{78} = 8.6 Hz, "H_8″ ArH), 7.89 (1H, d, J_{48} = 0.8 Hz, "H_4″ ArH), 7.51 (1H, d, J_{57} = 1.6 Hz, "H_5″ ArH), 7.48 (1H, dd, J_{57} = 1.59 Hz and J_{78} = 8.6 Hz, "H_7″ ArH), 7.12–7.41 (5H, m, ArH), 6.12 (2H, s, N-CH_2), 4.55 (2H, s, CH_2 of benzyl), 2.31 (3H, s, CH_3). ^{13}C NMR (100 MHz, DMSO-d_6, δ ppm): 154.82, 149.56, 147.48, 136.81, 136.54, 136.21, 131.45, 130.82, 129.78, 129.55, 129.03, 128.71, 127.55, 126.41, 54.82, 36.80, 23.67. Calcd Mass 381.88 MS (*m/z*): 383.08 (M^{+2}), 381.08 (M^+). Anal. Calcd for $C_{19}H_{16}N_5SCl$: C, 58.77; H, 3.84; N, 19.04. Found: C, 58.76; H, 3.89; N, 19.05.

4.2.6.19. 3-[(5-(Benzylthio)-1H-tetrazol-1-yl)methyl]-6-bromo-2-chloroquinoline ***7p***. Yellow solid; Yield: 78%, m.p. 138–140 °C; IR (KBr, cm^{-1}): 3065 (C-H), 1618 (C═N), 1593 (C═C), 721 (C-S). ^1H NMR (400 MHz, DMSO-d_6, δ ppm): 8.56 (1H, d, J_{78} = 8.6 Hz, "H_8″ ArH), 7.91 (1H, d, J_{48} = 1.2 Hz, "H_4″ ArH), 7.84 (1H, d, J_{57} = 1.6 Hz, "H_5″ ArH), 7.59 (1H, dd, J_{57} = 1.6 Hz and J_{78} = 8.6 Hz, "H_7″ ArH), 7.13–7.46 (5H, m, ArH), 6.11 (2H, s, N-CH_2), 4.50 (2H, s, CH_2 of benzyl). ^{13}C NMR (100 MHz, DMSO-d_6, δ ppm): 154.61, 149.55, 147.60, 136.89, 133.41, 131.48, 130.61, 129.97, 129.62, 129.18, 128.71, 128.45, 127.89, 117.75, 56.42, 36.87. Calcd Mass 446.75 MS (*m/z*): 448.97 (M^{+4}), 446.97 (M^{+2}), 444.98 (M). Anal. Calcd for $C_{18}H_{13}N_5SBrCl$: C, 47.19; H, 2.56; N, 16.18. Found: C, 47.20; H, 2.57; N, 16.15.

4.2.6.20. 3-[(5-(Benzylthio)-1H-tetrazol-1-yl)methyl]-2-chloro-6-fluoroquinoline ***7q***. Pale yellow solid; Yield: 72%, m.p. 140–142 °C; IR (KBr, cm^{-1}): 3060 (C-H), 1591 (C═N), 1567 (C═C), 718 (C-S). ^1H NMR (400 MHz, DMSO-d_6, δ ppm): 8.59 (1H, d, J_{78} = 8.4 Hz, "H_8″ ArH), 8.24 (1H, d, J_{48} = 0.8 Hz, "H_4″ ArH), 7.86 (1H, d, J_{57} = 1.4 Hz, "H_5″ ArH), 7.61 (1H, dd, J_{57} = 1.4 Hz and J_{78} = 8.4 Hz, "H_7″ ArH), 7.17–7.48 (5H, m, ArH), 6.08 (2H, s, N-CH_2), 4.52 (2H, s, CH_2 of benzyl). ^{13}C NMR (100 MHz, DMSO-d_6, δ ppm): 154.43, 149.48, 147.81, 136.78, 130.64, 129.81, 129.39, 129.14, 128.85, 128.21, 127.56, 127.32, 121.45, 111.43, 55.71, 36.81. Calcd Mass 385.85 MS (*m/z*): 387.05 (M^{+2}), 385.06 (M^+). Anal. Calcd for $C_{18}H_{13}N_5SFCl$: C, 54.91; H, 2.98; N, 18.84. Found: C, 54.89; H, 2.97; N, 18.87.

5. Bioassay conditions

5.1. Molecular docking

5.1.1. DNA ligand docking

The crystal structure used were, (PDB ID: 453D), B-DNA [(5′-D(*CP*GP* CP* GP*AP*AP*TP*TP*CP*GP*CP*G)-3'-benzimidazole complex)] [61] and solution structure of intrastrand cisplatin-cross linked DNA octamer (PDB ID: 1AU5), D(CCTG*G*TCC): D(GGA CCAGG), NMR, minimized average structure [62], obtained from the Protein Data Bank (www.rcsb.org/pdb). The DNA file was prepared for docking by adding polar hydrogen atom with Gasteiger-Huckel charges and water molecules were removed. The 3D structure of the ligands was generated by the SKETCH module and was implemented in the SYBYL program (Tripos Inc., St. Louis, USA). The energy-minimized conformation was obtained with the help of the Tripos force field using the Gasteiger-Huckel [63] charges. The molecular docking was performed with the Surflex-Dock program which was interfaced with Sybyl-X 2.0 [64]. Later the other miscellaneous parameters were assigned to the default values given by the software.

5.1.2. NMT, DHFR docking with ligand

The protein crystal structure file NMT *Aspergillus fumigatus* and DHFR *Candida albicans* (PDB ID: 4CAW; B-Chain and 1AI9), was taken from PDB (www.rcsb.org/pdb). The proteins were prepared for docking by adding polar hydrogen atom with Gasteiger-Huckel charges and water molecules were removed. The 3D structure of the ligands was generated by the SKETCH module implemented in the SYBYL program (Tripos Inc., St. Louis, USA) and its energy-minimized conformation was obtained with the help of the Tripos force field using Gasteiger-Huckel [63] charges and molecular docking was performed with Surflex-Dock program that is interfaced with Sybyl-X 2.0 [64] and other miscellaneous parameters were assigned with the default values given by the software.

5.2. In vitro anticancer screening

All the human tumor cell lines for the cancer screening panel were grown in RPMI 1640 medium containing 5% fetal bovine serum and 2 mM l-glutamine. The typical screening experiment is carried out by inoculating the cells into 96 well microtiter plates in 100 μl with plating densities ranging from 5000 to 40,000 cells/well, which depends on the doubling time of individual cell lines. After inoculation, the microtiter plates were incubated at 37 °C, 5% CO_2, 95% air and 100% relative humidity for 24 h prior to addition of experimental drugs. After 24 h, two of the plates of each cell line were fixed *in situ* with TCA, to represent the measurement of the cell population for each cell line at the time of drug addition (*Tz*). Experimental drugs were solubilized in dimethyl sulfoxide at around 400-folds and the desired final maximum test concentration was stored frozen prior to use. At the time of drug addition, an aliquot of frozen concentrate is defrosted and diluted to twice the desired final maximum test concentration with the complete medium containing 50 μg/ml Gentamicin. An additional, 10-fold of serial dilutions were added to a total of five drug concentrations plus control. Aliquots of 100 μl of these different drug dilutions were added to the appropriate microtiter wells, containing 100 μl of medium, resulting in the required final drug concentrations.

Following drug addition, all the plates were incubated for an additional 48 h at 37 °C, 5% CO_2, 95% air, and 100% relative humidity. For adherent cells, the assay was terminated by the addition of cold TCA. Cells were fixed *in situ* by the gentle addition of 50 μl of cold 50% (w/v) TCA (final concentration, 10% TCA) and incubated for about 60 min at 4 °C. The supernatant was discarded, and the plates were washed five times with tap water and air dried. Sulforhodamine B (SRB) solution (100 μl) at 0.4% (w/v) in 1% acetic acid was added to each well, and the plates were incubated for 10 min at room temperature. After staining, unbound dye was removed by washing five times with 1% acetic acid and the plates were air dried. Bound stain was thoroughly solubilized with 10 mM trizma base, and the absorbance was read on an automated plate reader at a wavelength of 515 nm. For suspension cells, the methodology was the same except that the assay was terminated by fixing settled cells at the bottom of the wells by adding 50 μl of 80% TCA (final concentration, 16% TCA). Using the seven absorbance measurements [time zero, (*Tz*), control growth, (*C*), and test growth in the presence of drug at the five concentration levels (*Ti*)], the percentage growth is calculated at each of the drug concentrations levels. Percentage growth inhibition is calculated as:

$$[(Ti - Tz)/(C - Tz)] \times 100 \text{ for concentrations for which } Ti > / = Tz$$

$$[(Ti - Tz)/Tz] \times 100 \text{ for concentrations for which } Ti < Tz$$

Three dose response parameters were calculated for each experimental agent. Growth inhibition of 50% (GI_{50}) was calculated from $[(Ti\text{-}Tz)/(C\text{-}Tz)] \times 100 = 50$, which the drug concentration resulting in a 50% reduction in the net protein increase (as measured by SRB staining) in control cells during the drug incubation. The drug concentration resulting in total growth inhibition (TGI) was calculated from $Ti = Tz$. The LC_{50} (concentration of drug resulting in a 50% reduction in the measured protein at the end of the drug treatment as compared to that at the beginning) indicating a net loss of cells following treatment was calculated from $[(Ti\text{-}Tz)/Tz] \times 100 = -50$. Values were calculated for each of these three parameters if the level of activity was reached; however, if the effect was not reached or exceeded, the value for that parameter was expressed as greater or less than the maximum or minimum concentration tested [65,66].

5.3. *In vitro* antifungal activity

The title compounds were evaluated for their *in vitro* antifungal activity with *C. albicans* and *A. fumigatus* (cultured) by Disc Diffusion Method [67] with Sabouraud agar medium. Fluconazole was used as a reference drug. Each compound was tested at a concentration of 100 μg/ml in DMSO. The zone of inhibition (mm) was measured at 37 °C. Briefly, agar (pH = 7.2–7.4) was placed into Petri dish (100 mm size and 4 mm depth). The agar plates were then inoculated with broth cultures diluted to McFarland 0.5 turbidity. A disc containing known amounts of a compound to be analyzed was placed on the surface of an agar plate that has been inoculated with a standardized suspension of microorganisms to be tested. Paper discs with only DMSO (tests involving Fluconazole) were used as negative controls. All experiments were conducted in triplicate and repeated if the results differed.

Dilutions of each drug have to be done with BHI for MIC [68]. In the initial tube 20 μL of drug was added into the 380 μL of BHI broth. For dilutions 200 μL of BHI broth was added into the next 9 tubes separately. Then from the initial tube 200 μL was transferred to the first tube containing 200 μL of BHI broth. This was considered as 10^{-1} dilution. From 10^{-1} diluted tube 200 μL was transferred to second tube to make 10^{-2} dilution. The serial dilution was repeated up to 10^{-9} dilution for each drug. From the maintained stock cultures of required organisms, 5 μL was taken and added into BHI (2 mL) broth. In each serially diluted tube 200 μl of above culture suspension was added. The tubes were incubated for 24 h and observed for turbidity. The MIC values were obtained from the lowest concentration of the test compounds where the tubes remained clear indicating that the bacterial or fungal growth was completely inhibited at this concentration.

Conflict of interest

The authors have declared no conflicts of interest.

Acknowledgements

The authors are grateful to NCI, NIH, Bethesda, USA for selecting samples for *in vitro* anticancer analyses under DTP. The authors acknowledge the NGH College of Dental Sciences Belgaum, Karnataka, India for antifungal activity. The authors wish to thank the University Science Instrumentation Centre (USIC), Karnataka University, Dharwad, NMR Research Centre, Indian Institute of Science (IISc), Bengaluru, India for carrying out the X-ray, spectral analyses and Dr. V. H. Kulkarni, Principal, S. E. T's College of Pharmacy, Dharwad, India for docking studies. The authors are also thankful to UGC, New Delhi for providing financial assistance under UGC-UPE thrust area "Antitumor activity: An Integrated Approach" vide [F.No. 14-3/2012(NS/PE) Dated: 14-03-2012]. One of the authors (SKJS) acknowledges UGC, New Delhi, India for awarding RFSMS fellowship vide [F.25-1/2013-14(BSR)/7–100/2007(BSR), Dated 30/05/2014].

Appendix A. Supplementary data

Supplementary data related to this article can be found at http://dx.doi.org/10.1016/j.ejmech.2017.01.043.

References

[1] B. Stewart, P. Kleihues (Eds.), World Cancer Report (World Health Organization, International Agency for Cancer Research), IARC Press, Lyon, 2003.
[2] D.M. Parkin, Global cancer statistics in the year 2000, Lancet Oncol. 2 (2001) 533–543.
[3] N. Beaulieu, D. Bloom, R. Bloom, R. Stein, Breakaway: the Global Burden of Cancer Challenges and Opportunities, The Economist Intelligence Unit, 2009.
[4] P. Ribaud, Fungal infections and the cancer patient, Eur. J. Cancer 33 (1997) 50–54.
[5] C. Sheng, W. Zhang, Review: new lead structures in antifungal drug discovery, Curr. Med. Chem. 18 (2011) 733–766.
[6] V.R. Solomon, H. Lee, Quinoline as a privileged scaffold in cancer drug discovery, Curr. Med. Chem. 18 (2011) 1488–1508.
[7] J.M. Fostel, P.A. Lartey, Emerging novel antifungal agents, Drug. Discov. Today 5 (2000) 25–32.
[8] D. Zainaba, L. Meryem, B. Abdelmejid, A. Abdelfatah, H. Mohammed, K. Said, B. Mohammed, Antileishmanial activity of a new 8-hydroxyquinoline derivative designed 7-[5'-(3'-phenylisoxazolino) methyl]-8-hydroxyquinoline: preliminary study, FARMACO 59 (2004) 195–199.
[9] J. Jampilek, M. Dolezal, J. Kunes, V. Buchta, L. Silva, K. Kralova, Quinaldine derivatives: preparation and biological activity, Med. Chem. 1 (2005) 591–599.
[10] M. K. Majerz, B. Oleksyn, R. Musiol, B. Podeszwa, J. Polanski, Abstracts of Papers, Joint Meeting on Medicinal Chemistry, Vienna, Austria, June 20-23, 2005, Intl. Sci. Pharm. 73 (2005) 194.
[11] J.M. Urbina, J.C.G. Cortes, A. Palma, S.N. Lopez, S.A. Zacchino, R.D. Enriz, J.C. Ribas, V.V. Kouznetsov, Inhibitors of the fungal cell wall, synthesis of 4-aryl-4- N-arylamine-1-butenes and related compounds with inhibitory activities on (1–3) glucan and chitin synthesis, Bioorg. Med. Chem. 8 (2000) 691–698.
[12] S.D. Joshi, U.A. More, D. Parkale, T.M. Aminabhavi, A.K. Gadad, M.N. Nadagouda, R. Jawarkar, Design, synthesis of quinolinyl Schiff bases and azetidinones as enoyl ACP-reductase inhibitors, Med. Chem. Res. 24 (2015) 3892–3911.
[13] S. Vangapandu, M. Jain, R. Jain, S. Kaur, P.P. Singh, Ring-substituted quinolines as potential anti-tuberculosis agents, Bioorg. Med. Chem. 12 (2004) 2501–2508.
[14] M.V. de Souza, K.C. Pais, C.R. Kaiser, M.A. Peralta, L.M. de Ferreira, M.C. Lourenço, Synthesis and *in vitro* antitubercular activity of a series of quinoline derivatives, Bioorg. Med. Chem. 17 (2009) 1474–1480.
[15] H. Cope, R. Mutter, W. Heal, C. Pascoe, P. Brown, S. Pratt, Synthesis and SAR study of acridine, 2-methylquinoline and 2-phenylquinazoline analogues as anti-prion agents, Eur. J. Med. Chem. 41 (2006) 1124–1143.
[16] C.H. Tseng, Y.L. Chen, P.J. Lu, C.N. Yang, C.C. Tzeng, Synthesis and antiproliferative evaluation of certain Indeno[1,2-*c*]quinoline derivatives, Bioorg. Med. Chem. 16 (2008) 3153–3162.
[17] S.B. Marganakop, R.R. Kamble, T. Taj, M.Y. Karidurganvar, An efficient one-pot cyclization of quinoline thiosemicarbazones to quinolines derivatized with 1,3,4- thiadiazoles as anticancer and anti-tubercular agents, Med. Chem. Res. 21 (2012) 185–191.
[18] F. Pisaneschi, Q.D. Nguyen, E. Shamsaei, M. Glaser, E. Robins, M. Kaliszczak, G. Smith, A.C. Spivey, E.O. Aboagye, Development of a new epidermal growth factor receptor positron emission tomography imaging agent based on the 3-cyanoquinoline core: synthesis and biological evaluation, Bioorg. Med. Chem. 8 (2010) 6634–6645.
[19] Y. Wang, J. Ai, Y. WangChen, L. Wang, G. Liu, M. Geng, A. Zhang, Synthesis and c-Met kinase inhibition of 3,5-disubstituted and 3,5,7-trisubstituted quinolines: identification of 3-(4 acetylpiperazin-1-yl)-5-(3-nitrobenzylamino)-7 (trifluoromethyl) quinoline as a novel anticancer agent, J. Med. Chem. 54 (2011) 2127–2142.
[20] M.G. Ferlin, B. Gatto, G. Chiarelotto, M. Palumbo, Pyrrolo-quinoline derivatives as potential antineoplastic drugs, Bioorg. Med. Chem. 8 (2000) 1415–1422.
[21] V. Moret, Y. Laras, T. Cresteil, G. Aubert, D.Q. Ping, C. Di, M.B. Requin, C. B'eclin, V. Peyrot, D. Allegro, A. Rolland, F.D. Angelis, E. Gatti, P. Pierre, L. Pasquini, E. Petrucci, U. Testa, J.L. Kraus, Discovery of a new family of bis-8- hydroxyl quinoline substituted benzylamines with pro-apoptotic activity in cancer cells: synthesis, structure-activity relationship, and action mechanism studies, Eur. J. Med.Chem. 44 (2009) 558–567.
[22] A.M. Rashad, W.A. El-Sayed, A.M. Mohamed, M.M. Ali, Synthesis of new quinoline derivatives as inhibitors of human tumor cells growth, Arch.

Pharm.Chem. Life. Sci. 343 (2010) 440–448.
[23] R.K. Arafa, G.H. Hegazy, G.A. Piazza, A.H. Abadi, Synthesis and *in vitro* anti-proliferative effect of novel quinolone-based potential anticancer agents, Eur. J. Med. Chem. 63 (2013) 826–832.
[24] S.S. Chhajed, P. Manicha, V.A. Bastikar, H. Animeshchandra, V.N. Ingle, C.D. Upasani, S.S. Wazalwar, Synthesis and molecular modeling studies of 3-chloro-4- substituted-1-(8-hydroxy-quinolin-5-yl)-azetidin-2-ones as novel anti-filarial agents, Bioorg. Med. Chem. Lett. 20 (2010) 3640–3644.
[25] J. Polanski, H. Niedbala, R. Musiol, B. Podeszwa, D. Tabak, A. Palka, A. Mencel, J.F. Finster, M.L.B. Mouscadet, 5-Hydroxy-6-quinaldic acid as a novel molecular scaffold for HIV-1 integrase inhibitors, Lett. Drug. Des. Discov. 3 (2006) 175–178.
[26] R. Musiol, M. Serda, S.H. Bielowka, J. Polanski, Quinoline-based antifungals, Curr. Med. Chem. 17 (2010) 1960–1973.
[27] M. Shekarchi, M.B. Marvasti, M. Sharifzadeh, A. Shafiee, Iran. J. Pharm. Res. 1 (2005) 33–36.
[28] M.S. Mohamed, R.A. El-Domany, R.H. Abd El-Hameed, Synthesis of certain pyrrole derivatives as antimicrobial agents, Acta. Pharm. 59 (2009) 145–158.
[29] H.N. Patil, D. Varadaraji, S.S. Suban, V.R. Ramasamy, K. Kubendiran, K. Jai Sankar, G. Raguraman, S.K. Nalilu, Synthesis and evaluation of a series of 1-substituted tetrazole derivatives as antimicrobial agents, Org. Commun. 33 (2010) 45–56.
[30] A.A. Bekhita, Ola A. El-Sayed, E. Aboulmagd, J.Y. Park, Tetrazolo [1,5-*a*] quinoline as a potential promising new scaffold for the synthesis of novel anti inflammatory and antibacterial agents, Eur. J. Med. Chem. 39 (2004) 249–255.
[31] A.H. Said El-Feky, K.Z. Abd El-Samii, N.A. Osman, J. Lashine, M.A. Kamel, H.K. Thabet, Synthesis, molecular docking and anti-inflammatory screening of novel quinoline incorporated pyrazole derivatives using the Pfitzinger reaction II, Biorg. Chem. 58 (2015) 104–116.
[32] A. Rajasekaran, K.A. Rajagopal, Synthesis of some novel triazole derivatives as anti- nociceptive and anti-inflammatory agents, Acta. Pharm. 59 (2009) 355–364.
[33] A. Rajasekaran, P.P. Thampi, Synthesis and antinociceptive activity of some substituted-{5-[2-(1, 2, 3, 4-tetrahydrocarbazol-9-yl) ethyl] tetrazol-1-yl} alkanones, Eur. J. Med. Chem. 40 (2005) 1359–1364.
[34] V.H. Bhaskar, P.B. Mohite, Synthesis, characterization and evaluation of anti-cancer activity of some tetrazole derivatives, J. Optoelectron. Biomed Mater. 2 (2010) 249–259.
[35] M. Arshad, A.R. Bhat, S. Pokharel, J.E. Kim, E.J. Lee, F. Athar, I. Choi, Synthesis, characterization and anticancer screening of some novel piperonyletetrazole derivatives, Eur. J. Med. Chem. 71 (2014) 229–236.
[36] L. Navidopour, M. Amni, H. Shafarwoodi, K.J. Abdi, M.H. Ghahremani, A. Shafiee, Design and synthesis of new water soluble tetrazolide derivatives of celecoxib and rofecoxib as selective cyclooxygenase-2 (COX-2) inhibitors, Bioorg. Med. Chem. Lett. 15 (2006) 4483–4487.
[37] Y.L. Gao, G.L. Zhao, W. Liu, H. Shao, Y.L. Wang, W.R. Xu, L.D. Tangand, J.W. Wang, Design, Synthesis and in vivo hypoglycemic activity of tetrazole bearing N- glycosides as SGLT2 inhibitors, Ind. J. Chem. 49B (2010) 1499–1508.
[38] C. Liljebris, S.D. Larsen, D. Ogg, B.J. Palazuk, J.E. Bleasdale, Investigation of potential bioisosteric replacements for the carboxyl groups of peptidomimetic inhibitors of protein tyrosine phosphatase 1B: identification of a tetrazole-containing inhibitor with cellular activity, J. Med. Chem. 45 (2002) 1785–1798.
[39] a) R.D. Taylor, M. MacCoss, A.D.G. Lawson, J. Med. Chem. 57 (2014) 5845–5859;
b) N. Tsuchimori, R. Hayashi, N. Kitamoto, K. Asai, T. Kitazaki, Y. Iizawa, K. Itoh, K. Okonogi, Antimicrob. Agents. Chemother. 46 (2002) 1388–1393.
[40] X.Y. Meng, H.X. Zhang, M. Mezei, M. Cui, Molecular Docking: a powerful approach for structure-based drug discovery, Curr. Comput. Aided. Drug. Des. 7 (2011) 146–157.
[41] Y. Gilad, H. Senderowitz, Docking studies on DNA intercalators, J. Chem. Inf. Model 54 (2014) 96–107.
[42] A. Rescifina, C. Zagni, M.G. Varrica, V. Pistarà, A. Corsaro, Recent advances in small organic molecules as DNA intercalating agents: synthesis, activity, and modeling, Eur. J. Med. Chem. 74 (2014) 95–115.
[43] J.A. Boutin, Myristoylation, Cell. Signal 9 (1997) 15–35.
[44] T.A. Farazi, G. Waksman, J.I. Gordon, The biology and enzymology of protein *N*- myristoylation, Biol. Chem. 276 (2001) 39501–39504.
[45] J.K. Lodge, R.L. Johnson, R.A. Weinberg, J.I. Gordon, Comparison of myristoyl-CoA:protein *N*-myristoyltransferases from three pathogenic fungi: cryptococcus neoformans, Histoplasma capsulatum and Candida albicans, J. Biol. Chem. 269 (1994) 2996–3009.
[46] C. Zhao, S. Ma, Recent advances in the discovery of *N*-Myristoyltransferase inhibitors, Chem. Med. Chem. 9 (2014) 2425–2437.
[47] B. Roth, C.C. Cheng, Recent progress in the medicinal chemistry of 2,4-diamino pyrimidines, Prog. Med. Chem. 19 (1982) 269–331.
[48] R.A. Castaldo, D.W. Gump, J.J. McCormack, Activity of 2, 4-diaminoquinazoline compounds against Candida species, Antimicrob. Agent Chemother. 15 (1979) 81–86.
[49] J.H. Chan, J.S. Hong, L.F. Kuyper, D.P. Baccanari, S.S. Joyner, R.L. Tansik, C.M. Boytos, S.K. Rudolpht, Selective inhibitors of *Candida albicans* dihydrofolate reductase: activity and selectivity of 5-(Arylthio)-2, 4-diaminoquinazolines, J. Med. Chem. 38 (1995) 3608–3616.
[50] A.E. Rashad, W.A. El-Sayed, A.M. Mohamed, M.M. Ali, Synthesis of new quinoline derivatives as inhibitors of human tumor cells growth, Arch. Pharm. Chem. Life Sci. 8 (2010) 440–448.
[51] F.A. Bassyouni, S.M. AbuBaker, K. Mahmoud, M. Moharam, S.S. El- Nakkady, Rehim, Synthesis and biological evaluation of some new triazolo[1,5-*a*]quinoline derivatives as anticancer and antimicrobial agents, RSC Adv. 4 (2014) 24131–24141.
[52] R.B. Uttarwar, R.B. Nawale, P.B. Shamkuwar, Synthesis and pharmacological screening of derivatives of benzimidazole linked with quinoline and tetrazole, J. Chem. Pharm. Res. 5 (2013) 41–46.
[53] A.A. Bekhita, Ola A. El-Sayed, E. Aboulmagd, J.Y. Park, Tetrazolo [1, 5-*a*] quinoline as a potential promising new scaffold for the synthesis of novel anti inflammatory and antibacterial agents, Eur. J. Med. Chem. 39 (2004) 249–255.
[54] F.H. Allen, C.R. Groom, J.W. Liebeschuetz, D.A. Bardwell, T.S.G. Olsson, P.A. Wood, The hydrogen bond environments of 1*H*-tetrazole and tetrazolate rings: the structural basis for tetrazole–carboxylic acid bioisosterism, J. Chem. Inf. Model 52 (2012) 857–866.
[55] B. Ledoussal, J.K. Almstead, C.P. Flaim, Novel fluoroquinolone, structure activity, and design of new potent and safe agents, in: Program and Abstracts of the 39th Interscience Conference on Antimicrobial Agents and Chemotherapy (San Francisco), American Society for Microbiology, Washington, DC, 1999.
[56] J. Yin, S.L. Buchwald, Palladium-catalyzed intermolecular coupling of aryl halides and amides, Org. Lett. 2 (2000) 1101–1104.
[57] G.Y. Zhang, N-(5-Methyl-sulfanyl-1, 3, 4- thia-diazol-2-yl) acetamide, Acta Cryst. Sec E. 65 (2009) 2138.
[58] http://dtp.nci.nih.gov/docs/compare/compare.html.
[59] L.R. Peterson, Quinolone molecular structure-activity relationships: what we have learned about improving antimicrobial activity, Clin. Infect. Dis. 33 (2001) 180–186.
[60] M.Q. Zhang, M.E. Zwaagstra, Structural requirements of luekotriene *CysT1* receptor ligands, Curr. Med. Chem. 4 (1997) 229–242.
[61] H.M. Berman, J. Westbrook, Z. Feng, G. Gilliland, T.N. Bhat, H. Weissig, I.N. Shindyalov, P.E. Bourne, The protein data bank, Nucl. Acids Res. 28 (2000) 235–242.
[62] Y. Gilad, H. Senderowitz, Docking studies on DNA intercalators, J. Chem. Inf. Model 54 (2014) 96–107.
[63] J. Sambrook, E.F. Fritsch, T. Maniatis, Molecular Cloning, a Laboratory Manual, second ed., Cold Spring Harbor Laboratory, Cold Spring Harbor, New York, 1989.
[64] J. Gasteiger, M. Marsili, Iterative partial equalization of orbital electronegativity-a rapid access to atomic charges, Tetrahedron 36 (1980) 3219–3228.
[65] M.R. Boyd, K.D. Paull, Some practical consideration and applications of the NCI *in vitro* drug discovery screen, Drug Dev. Res. 34 (1995) 91–109.
[66] M.R. Grever, S.A. Schepartz, B.A. Chabner, The National Cancer Institute: cancer drug discovery and development program, Semin. Oncol. 19 (1992) 622–638.
[67] H.D. Isenberg, Clinical Microbiology Procedures Handbook, vol. 1, American society for microbiology/Washington, D.C., 1992.
[68] R. Schwalve, L.S. Moore, A.C. Goodwin, Antimicrobial Susceptibility Testing Protocols, Crc. Press, Taylor and Francis, 2007.